Mechanical Systems and Signal Processing 177 (2022) 109121

Contents lists available at ScienceDirect

Mechanical Systems and Signal Processing

journal homepage: www.elsevier.com/locate/ymssp

An analytical framework for broadband dynamic analysis of plate built-up structures with uncertain viscoelastic boundary or connection conditions

Xiao Liu [a,b,c], Xiang Liu [a,b,c,*], Sondipon Adhikari [d], Xueyi Zhao [a,b,c]

[a] Key Laboratory of Traffic Safety on Track, Ministry of Education, School of Traffic & Transportation Engineering, Central South University, Changsha, China
[b] Joint International Research Laboratory of Key Technology for Rail Traffic Safety, Central South University, Changsha, China
[c] National & Local Joint Engineering Research Center of Safety Technology for Rail Vehicle, Central South University, Changsha, China
[d] James Watt School of Engineering, The University of Glasgow, Glasgow G12 8QQ, United Kingdom

ARTICLE INFO

Communicated by J.E. Mottershead

Keywords:
Stochastic spectral dynamic stiffness method
Karhunen–Loève expansion
Stochastic broadband dynamic analysis
Built-up structures
Uncertain boundary and connection conditions

ABSTRACT

This paper proposes an analytical stochastic spectral dynamic stiffness method (SSDSM) for free and forced vibration analysis of plate built-up structures subject to uncertain viscoelastic boundary or connection conditions (BCs or CCs). First, a recently developed spectral dynamic stiffness (SDS) theory for broadband vibration analysis of plate built-up structure with arbitrary spatially-varying viscoelastic BCs or CCs is extended to model deterministic viscoelastic BCs or CCs. Then, uncertain viscoelastic BCs or CCs are described by random fields in stiffness and damping, which are discretized by Karhunen–Loève expansion. By using the modified Fourier series as the shape functions for the BCs or CCs, the analytical SSDS matrices of the uncertain viscoelastic BCs or CCs are developed. Then, those SSDS matrices are superposed directly to the SDS matrix of the plate built-up structure. For the solution technique, the extended Wittrick–Williams algorithm is used for stochastic eigenvalue analysis, whereas two different methods are proposed for stochastic response analysis. Representative examples are chosen to validate and demonstrate the superiorities of the proposed method. The proposed method retains all the advantages of the SDS method which is highly efficient and accurate within the whole frequency range. Meanwhile, the proposed method also provides a feasible technique for stochastic broadband dynamic analysis of plate-like structures subject to uncertain boundary or connection conditions.

1. Introduction

Plate-like structures with arbitrary spatially-varying viscoelastic supports (Fig. 1(a)) and viscoelastic coupling constraints (Fig. 1(b)) are widely encountered in engineering. Their application scopes include but not limited to bridges, automobiles, airplanes, ships, buildings, high-speed trains, machines and other structures [1,2]. The design of boundary and connection conditions for plate built-up structures usually involves both mechanical fastening and adhesive bonded fastening types [3]. There are two main reasons that the mechanical parameters for boundary and connection conditions can be described by random fields. On the one hand, due to

* Corresponding author at: Key Laboratory of Traffic Safety on Track, Ministry of Education, School of Traffic & Transportation Engineering, Central South University, Changsha, China.
E-mail addresses: xiaoliu11@csu.edu.cn (X. Liu), xiangliu06@gmail.com (X. Liu), Sondipon.Adhikari@glasgow.ac.uk (S. Adhikari), zxy563675400@csu.edu.cn (X. Zhao).

https://doi.org/10.1016/j.ymssp.2022.109121
Received 30 November 2021; Received in revised form 23 February 2022; Accepted 30 March 2022
Available online 27 April 2022

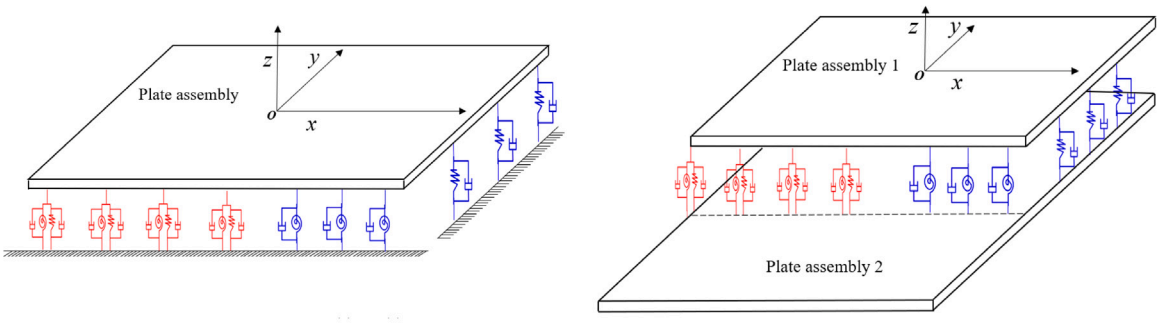

(a) Viscoelastic supports (b) Viscoelastic coupling constraints

Fig. 1. Two general types of spatially-varying boundary and connection conditions covered by the theory of this paper: (a) Viscoelastic supports with non-uniform translational and rotational stiffnesses and damping with uncertainties (b) Viscoelastic coupling constraints with non-uniform translational and rotational coupling stiffnesses and damping with uncertainties.

the level of craftsmanship in the assembly and manufacturing process, not all boundary and connection conditions for structures can meet the design requirements of the fastening standards, and the mechanical properties could be non-uniformed and uncertain. On the other hand, fatigue due to cyclic loading and material aging can also cause loosening of boundary and connection conditions. For vibration problems, boundary and connection conditions in engineering can be generally modeled as linear models characterized by spatially distributed stiffness and damping models. Therefore, the stiffness and damping models can be regarded as random fields in practical engineering problems. The boundary and connection conditions with uncertainties of the plate structures may not only decrease the constraint strength and local stiffness but also increase interface abrasion and the probability of structural fatigue failures. More importantly, the boundary or connection conditions play a significant role in the dynamic behaviors of plate built-up structures. Therefore, those uncertainties must be considered in the dynamic analysis. The safety factor method is applied in the analysis and designs to avoid this situation, but it often leads to either uneconomical or unsafe designs. In many high-end equipment manufacturing industries, it is increasingly necessary to consider the uncertainties of boundary and connection conditions in modeling to ensure the high fidelity of design [4–9].

It can be found that the vast majority of existing research on the uncertain boundary or connection conditions were modeled under the framework of the stochastic finite element method (SFEM) [10–18]. However, as the wavelength shrinks over the higher frequency range, finer mesh size is required to accurately represent the dynamic behavior, which increases the computational effort significantly. In addition, once the complex combination of multi-unit plates is involved, the low computational efficiency caused by the fine grid division seems to be a stumbling block for this method. Next, we review related work on plate dynamics subject to general boundary conditions (BCs) or connection conditions (CCs) with uncertainties.

A wide range of studies on the dynamic characteristics of plates with elastic supports have been reported (see Fig. 1(a)) [19–27], but there are few publications on elastic supports with uncertainties. Silva et al. [13] used the SFEM to establish the plate structure model and approximated the uncertainties of the boundaries by the Bayesian approximation error method, then proposed a damage identification method for plate structure members. Muhanna and Shahi [28] developed the interval finite element method by modeling all uncertain parameters of viscoelastic supports as intervals, which can be extended to the stochastic analysis of plate structures. Avalos et al. [29] extracted the stiffness matrix in the finite element model of the curved beam for the stochastic modeling considering the uncertainties of the boundary conditions. Ritto et al. [30] used the finite element method to discretize the Timoshenko beam model and studied the uncertainties of the elastic torsional stiffness with the parametric and non-parametric probability methods. However, most of the current works are only applicable to plates with uniform boundary conditions.

The stochastic dynamic analysis of plate assemblies with viscoelastic coupling constraints (see Fig. 1(b)) is even more challenging, and has received rather sporadic attention [3,31–35]. Abolfathi et al. [31] studied the influence of the uncertainties of the support stiffness on the vibration transfer function of the plate built-up structure, but it was limited to low- to mid-frequency ranges. Ibrahim and Pettit [3] combined fuzzy set theory with the finite element method to investigate the effect of uncertainties and relaxation of joints in the dynamic behavior of structural systems. Mignolet and Soize [33] used the Craig–Bampton substructure method to establish an average model with boundary conditions/coupling flexibility and used non-parametric modeling methods to model the uncertainties lying in the boundary conditions and connection conditions, but these methods seem to be restricted to the low-frequency range.

In contrast to the SFEM, the analytical method will not be affected by meshing and can provide very accurate dynamic analysis. The literature [19,20,23–25] gives a series of analytical methods for the free vibration of structures with deterministic boundary conditions and connection conditions, but they are usually limited to spatially constant. In practical engineering problems, arbitrary boundary and connection conditions with different spatially-varying mechanical parameters may be encountered. In recent years, the analytical methods of deterministic spatially non-uniform boundary conditions and connection conditions have also received a small amount of attention [36–39]. Rayleigh–Ritz method has been commonly used to describe the elastic boundary conditions in the equation of motion of structures, where different types of allowable functions are chosen, such as modified Fourier series,

Chebyshev polynomials, orthogonal polynomials through Gram–Schmidt process. However, there has been quite sporadic attention on the analytical methods for the spatially non-uniform boundary conditions and connection conditions with uncertainties [40]. Li et al. [40] represented the partial bolt loosening phenomenon using the artificial spring–damper technique and Jones-Nelson theory. However, it is not clear whether the method can be applied to built-up structures, and the computational efficiency also needs to be proved urgently. It is a difficult task to achieve highly efficient and highly accurate stochastic dynamic analysis of more complex plate assemblies with spatially non-uniform uncertain boundary conditions and connection conditions using existing methods.

A powerful alternative tool has shown great potential for stochastic dynamic analysis called the stochastic dynamic stiffness method [41,42]. The method is often referred to as an exact method as it is based on the exact general solution of the governing differential equations [43–55]. The method provides the results with higher model accuracy especially within mid-to high-frequency ranges when compared to the stochastic finite element or other approximate methods. The stochastic dynamic stiffness models not only have the merits of the dynamic stiffness method that is accurate for the whole frequency ranges by using very few DOFs but also incorporate the parameter uncertainties in the model to perform stochastic analysis. Based on these stochastic dynamic stiffness models, broadband dynamic analyses have been carried out for both beam structures [41,56,57] and membrane built-up structures [42]. However, when developing two-dimensional (2D) DS elements like plates, the dynamic stiffness method was restricted to Levy-type rectangular plates with one pair of opposite edges simply supported. Thus, it allowed only sinusoidal deformation in one direction (e.g., see [58–63]) which leads to two inevitable consequences. On one hand, it is an obstacle in applying more general boundary conditions other than the Levy-type boundary conditions. On the other hand, the plate elements can only be assembled in one-directional and there was no clear possibility of assembling elements in a more general manner. These are naturally serious restrictions because engineering structures are modeled as plate and other elemental assemblies in a quite general manner.

Against the above background, this paper proposes a novel method called the stochastic spectral dynamic stiffness method (SSDSM) for free and forced vibration analysis of plate-like structures subject to arbitrary uncertain viscoelastic boundary or connection conditions (BCs or CCs) as illustrated in Fig. 1. First, by considering the effect of boundary or connection damping, the spectral dynamic stiffness (SDS) matrices for any arbitrarily distributed deterministic viscoelastic supports or viscoelastic coupling constraints are formulated concisely based on SDS theory [42,64–67]. Then, both the stiffness and damping of viscoelastic supports or viscoelastic coupling constraints are characterized by a set of random fields and decomposed by Karhunen–Loève (KL) expansion [68]. The modified Fourier series is then used as the shape function to derive the analytical stochastic SDS (SSDS) formulations for uncertain viscoelastic BCs or CCs. The developed SSDS matrices are superposed directly onto the corresponding components of the SDS matrix of the plate-like structure. Then the final matrix with uncertain viscoelastic BCs or CCs which includes damping effect can be obtained. For the solution techniques, the stochastic eigenvalue analysis and dynamic response analysis of plate assembly can be performed for a wide frequency range by using the extended Wittrick–Williams (WW) algorithm and matrix inversion method, respectively. In particular for stochastic dynamic response analysis, an improved technique based on domain decomposition is used to facilitate the response analysis subjected to any form of excitations such as uniform loads and non-uniform loads. The numerical examples demonstrate the computational efficiency and accuracy within the whole frequency of the proposed method. This work presents major contributions to derive analytical SSDS formulations for stochastic dynamic analysis of the plate-like structures with uncertain BCs or CCs by combining the merits of both the KL spectral expansion and SDSM mentioned above. The proposed method also provides a feasible technique for stochastic broadband dynamic analysis of plate-like structures subject to uncertain BCs or CCs.

This paper is organized as follows. Section 2 briefly introduces the general framework of deterministic spectral dynamic stiffness formulation for a plate element as well as the spectral dynamic stiffness formulation for spatially-varying viscoelastic supports and viscoelastic coupling constraints. Section 3 presents the general theory of the stochastic spectral dynamic stiffness based on KL expansion of random fields, then the SSDS matrices of the uncertain viscoelastic supports and the viscoelastic coupling constraints are developed. In Section 4, the eigenvalue analysis and dynamic response analysis method based on the SSDS model for the uncertain BCs or CCs of the plate structure is proposed respectively. In Section 5, the proposed theory is validated by and compared with numerical results through Monte-Carlo simulation. Finally, significant conclusions are drawn in Section 6.

2. Deterministic spectral dynamic stiffness formulation for plates

The main purpose of this paper is to extend the recently developed SDSM [64–67] to any arbitrary non-uniform distributed BCs or CCs with uncertainties. Therefore, the basic framework of SDSM is briefly summarized below to provide the necessary background for the stochastic SDSM for uncertain spatially-varying viscoelastic supports and viscoelastic coupling constraints.

2.1. Review of deterministic spectral dynamic stiffness (SDS) formulation for a plate element

A rectangular Kirchhoff plate of dimension $2a \times 2b$ undergoing transverse free vibration is shown in Fig. 2. The transverse amplitude $W(x, y)$ is described by the frequency-dependent governing differential equation (GDE) as

$$\frac{\partial^4 W}{\partial x^4} + 2\frac{\partial^4 W}{\partial x^2 \partial y^2} + \frac{\partial^4 W}{\partial y^4} - \kappa W = 0 \tag{1}$$

where

$$\kappa = \frac{\rho h \omega^2}{D}, \quad D = \frac{E h^3}{12\left(1 - \nu^2\right)} \tag{2}$$

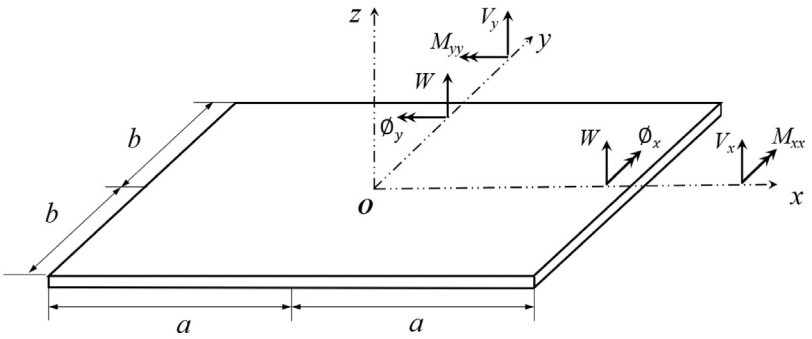

Fig. 2. Coordinate system and notations for displacement and forces for a thin plate.

and where ω is the circular frequency, hence κ is inertia related. D is the bending rigidity of the plate, E is the Young's modulus of material, ν is the Poisson ratio, h and ρ are respectively the thickness and mass density of the plate. The natural boundary conditions on the four plate edges can be derived through Hamilton's principle as follows the sign conventions illustrated in Fig. 2

$$\begin{aligned}
&\phi_x = -\frac{\partial W}{\partial x}; \quad \phi_y = -\frac{\partial W}{\partial y} \\
&M_x = -D\left(\frac{\partial^2 W}{\partial x^2} + \nu\frac{\partial^2 W}{\partial y^2}\right); \quad M_y = -D\left(\frac{\partial^2 W}{\partial y^2} + \nu\frac{\partial^2 W}{\partial x^2}\right) \\
&V_x = -D\left(\frac{\partial^3 W}{\partial x^3} + \Gamma^*\frac{\partial^3 W}{\partial x\partial y^2}\right); V_y = -D\left(\frac{\partial^3 W}{\partial y^3} + \Gamma^*\frac{\partial^3 W}{\partial y\partial x^2}\right)
\end{aligned} \tag{3}$$

where $\Gamma^* = 2-\nu$, ϕ_x and ϕ_y are the rotation of the transverse normals on the boundary about y and x axes respectively, M_x, M_y are bending moments and V_x, V_y are effective shear forces on the corresponding boundaries.

By using the spectral dynamic stiffness method (SDSM) [66], the general solution of the GDE of Eq. (1) for a plate element in the frequency domain can be obtained [64] based on the modified Fourier series [69]. Meanwhile, the modified Fourier series (in Appendix A) can also be used to describe any arbitrary displacement or force boundary conditions along the edges as given in Eq. (3) (line node r is used to represent x or y in local coordinates) of the plate. Then the SDS matrix for the plate element can be analytically formulated by substituting the above general solution into the general boundary conditions (BC) by some algebraic manipulation. In general, the analytical SDS formulation of a plate element can be developed which can be assembled to model plate assembly subject to arbitrary BCs or CCs [64,65,67]

$$\boldsymbol{f} = \boldsymbol{K}\boldsymbol{d}\,, \tag{4}$$

where $\boldsymbol{K}$ is the SDS matrix of the overall plate assembly, which relates the modified Fourier coefficient vector of the boundary forces $\boldsymbol{f}$ to that of the boundary displacements $\boldsymbol{d}$ on all of the boundaries (line nodes) of the plate assembly. $\boldsymbol{f}$ represents either V (V_x or V_y) or M (M_{xx} or M_{yy}) of Eq. (3) whereas $\boldsymbol{d}$ denotes either W or ϕ (ϕ_x or ϕ_y) of Eq. (3) on the corresponding boundaries. By using the SDSM, any arbitrary spatially-varying viscoelastic supports and viscoelastic coupling constraints along any line nodes (as shown in Fig. 1) can be successfully formulated following a similar framework of the SDSM.

2.2. Deterministic SDS formulation for arbitrarily spatially-varying viscoelastic boundary conditions (BCs) and connection conditions (CCs)

Next, it is necessary to revisit the spectral dynamic stiffness formulation for a plate with spatially-varying boundary conditions developed by the corresponding author [66]. This paper considers both spatially-varying damping and stiffness of the BCs or CCs whereas the previous work [66] was only for undamped supports or connections. In particular a SDS theory is developed for arbitrary spatially-varying viscoelastic supports (BCs) along any of the line nodes (Section 2.2.1) as well as any arbitrary spatially-varying viscoelastic coupling constraints (CCs) applied between any two line nodes (Section 2.2.2).

2.2.1. Development of the SDS formulation for viscoelastic supports

The SDS theory for viscoelastic supports (Fig. 1(a)) is developed with the Kirchhoff plate theory [66]. There are generally two types of generalized displacements along each plate line node, namely, the translational displacement $W(\mathrm{r})$ and the bending rotation $\phi(\mathrm{r})$; and the corresponding two generalized forces are the effective transverse shear force $V(\mathrm{r})$ and bending moment $M(\mathrm{r})$ respectively. For notational convenience, r is used in this paper to represent x or y which appears in Eq. (3). The viscoelastic supports applied on a certain line node (boundary) of the plate assembly will produce additional dynamic stiffness contributions during vibration. The additional generalized boundary forces induced by the viscoelastic supports can be written in the following form

$$V^a(\mathrm{r}) = [K_{\mathrm{w}}(\mathrm{r}) + \mathrm{i}C_{\mathrm{w}}(\mathrm{r})]W(\mathrm{r})\,, \tag{5a}$$

$$M^a(\mathrm{r}) = [K_{\phi}(\mathrm{r}) + \mathrm{i}C_{\phi}(\mathrm{r})]\phi(\mathrm{r})\,, \tag{5b}$$

Here, $K_w(r)$ and $K_\phi(r)$ are the translational and rotational stiffnesses of the viscoelastic supports along the line node $r \in [-L, L]$ (see Fig. 1(a)), whereas $C_w(r)$ and $C_\phi(r)$ are the translational and rotational damping of the viscoelastic supports along the line node (see Fig. 1(a)). All functions $K_w(r)$, $K_\phi(r)$, $C_w(r)$ and $C_\phi(r)$ can be arbitrarily specified, which can of course, be either uniform or non-uniform distributed. For notational convenience, the four equations in Eq. (5) can be expressed in a unified form as

$$f_i^a(r) = (\mu_K G_K(r) + i\mu_C G_C(r)) d_i(r), \quad r \in [-L, L], \tag{6}$$

where the subscript i denotes the ith line DOF on which the spatially-varying viscoelastic supports is applied. $\mu_K G_K(r) + i\mu_C G_C(r)$ represents the four spatially-varying functions in Eq. (5) respectively, namely, $K_w(r)$, $K_\phi(r)$, $C_w(r)$ and $C_\phi(r)$ which are applied onto the ith line DOF. $G_K(r)$ and $G_C(r)$ are *stiffness* and *damping dimensionless spatial functions* and μ is the *stiffness* or *damping constant*. Note that $\boldsymbol{f}_i$ and $\boldsymbol{d}_i$ in Eq. (4) are related by the corresponding component $\boldsymbol{K}_{ii}$ of the SDS matrix $\boldsymbol{K}$ given by Eq. (4) without considering viscoelastic supports or viscoelastic coupling constraints. Therefore, $\boldsymbol{K}_{ii}$ provides a linear mapping among the generalized force and displacement corresponding to all frequency–wavenumber dependent DOF of the ith line DOF. Next we need to formulate the additional SDS matrices $\boldsymbol{K}_{ii}^a$ of the viscoelastic supports which eventually will be superposed to $\boldsymbol{K}_{ii}$. $\boldsymbol{K}_{ii}^a$ has form as

$$\boldsymbol{K}_{ii}^a = \mu_K \boldsymbol{G}_K + i\mu_C \boldsymbol{G}_C. \tag{7}$$

based on the modified Fourier series [66], the *dimensionless SDS matrices* $\boldsymbol{G}_K$ and $\boldsymbol{G}_C$ are symmetric and the analytical expressions for those matrices corresponding to several typical spatial functions are given in [66].

The SDS matrix $\boldsymbol{K}_{ii}^a$ developed above for the viscoelastic supports along the ith *line DOF* is eventually superposed to the SDS matrix component $\boldsymbol{K}_{ii}$ to form the ii component of the final SDS matrix of the plate assembly $\boldsymbol{K}^{final}$ considering those supports and attachments to arrive at

$$\boldsymbol{K}_{ii}^{final} = \boldsymbol{K}_{ii} + \mu_K \boldsymbol{G}_K + i\mu_C \boldsymbol{G}_C. \tag{8}$$

2.2.2. Development of the SDS formulation for viscoelastic coupling constraints

In this section, we mainly discuss the ith and the jth line DOFs (along either boundaries or inter-element edges) of a plate assembly which are viscoelastically coupling constraints with non-uniform distributed coupling stiffness and damping $K(r) + iC(r)$. $K(r) + iC(r)$ stands for either translational or rotational coupling stiffness and damping, see Fig. 1(b). The coupling equation can be written in the following matrix form

$$\begin{bmatrix} f_i^a(r) \\ f_j^a(r) \end{bmatrix} = [K(r) + iC(r)] \begin{bmatrix} 1 & -1 \\ -1 & 1 \end{bmatrix} \begin{bmatrix} d_i(r) \\ d_j(r) \end{bmatrix}, \quad r \in [-L, L]. \tag{9}$$

where $d_i(r)$ and $d_j(r)$ are the generalized displacements for the ith and jth line DOFs respectively; $f_i^a(r)$ and $f_j^a(r)$ are the additional coupling forces acting on the corresponding line DOFs due to the coupling constraint $K(r) + iC(r)$. Similar to Eq. (7), the above coupling constraint stiffness function $K(r)$ and damping function $C(r)$ can also be written in the form

$$K(r) = \mu_K G_K(r), \quad C(r) = \mu_C G_C(r), \tag{10}$$

where μ_K and μ_C is the *dynamic stiffness constant* and *damping constant*, $G_K(r)$ and $G_C(r)$ are again, the corresponding dimensionless spatial function. Therefore, the first few steps of the SDS formulation for a non-uniform coupling constraint follow the same procedure for the previous viscoelastic supports. The main difference that will show up afterwards is that the forces of the two elastically coupled line DOFs are related to the two displacements as illustrated in Eq. (9). Consequently, the SDS matrix of a non-uniform viscoelastic coupling constraints for the elastically coupled two edges can be written in the form

$$\begin{bmatrix} \boldsymbol{f}_i^a \\ \boldsymbol{f}_j^a \end{bmatrix} = \left\{ \mu_K \begin{bmatrix} \boldsymbol{G}_K & -\boldsymbol{G}_K \\ -\boldsymbol{G}_K & \boldsymbol{G}_K \end{bmatrix} + i\mu_C \begin{bmatrix} \boldsymbol{G}_C & -\boldsymbol{G}_C \\ -\boldsymbol{G}_C & \boldsymbol{G}_C \end{bmatrix} \right\} \begin{bmatrix} \boldsymbol{d}_i \\ \boldsymbol{d}_j \end{bmatrix}, \tag{11}$$

where matrix $\boldsymbol{G}_K$ and $\boldsymbol{G}_C$ are the same as that of Eq. (7) but corresponds to the viscoelastic coupling stiffness and damping spatial function $G_K(r)$ and $G_C(r)$. Next, the sub-SDS matrices $\mu_K \boldsymbol{G}_K + i\mu_C \boldsymbol{G}_C$ in Eq. (11) are superposed directly to the frequency–wavenumber dependent DOFs (rows and columns) corresponding to the ith and jth line DOFs of the SDS matrix for the plate assembly resulting in

$$\begin{aligned} \boldsymbol{K}_{ii}^{final} &= \boldsymbol{K}_{ii} + \mu_K \boldsymbol{G}_K + i\mu_C \boldsymbol{G}_C, \quad \boldsymbol{K}_{jj}^{final} = \boldsymbol{K}_{jj} + \mu_K \boldsymbol{G}_K + i\mu_C \boldsymbol{G}_C, \\ \boldsymbol{K}_{ij}^{final} &= \boldsymbol{K}_{ij} - (\mu_K \boldsymbol{G}_K + i\mu_C \boldsymbol{G}_C), \quad \boldsymbol{K}_{ji}^{final} = \boldsymbol{K}_{ji} - (\mu_K \boldsymbol{G}_K + i\mu_C \boldsymbol{G}_C). \end{aligned} \tag{12}$$

Repeating the procedure described in Sections 2.2.1 and 2.2.2 and following Eqs. (8) and (12) for each viscoelastic supports and viscoelastic coupling constraints, the final deterministic SDS matrix of the complete structure is formulated. Once the SDS model of plate structure with determined boundary or connection conditions is established, the stochastic SDS model with uncertain BCs or CCs can be developed, which will be presented next.

3. Stochastic spectral dynamic stiffness (SSDS) formulation for spatially-varying viscoelastic boundary conditions (BCs) and connection conditions (CCs) with uncertainties

3.1. General theory for stochastic spectral dynamic stiffness method for uncertain BCs and CCs by using KL expansion

The uncertainties in specifying boundary condition (BCs) or connection conditions (CCs) of the structure are modeled within the framework of random fields. The $(\Theta, \mathcal{F}, P)$ can be considered as a probability space with $\theta \in \Theta$ denoting a sampling point in the sampling space Θ, $\mathcal{F}$ is the complete σ-algebra over the subsets of Θ and P is the probability measure. Suppose the spatial coordinate vector $\mathrm{r} \in \mathbb{R}^d$. Consider $H : \left(\mathbb{R}^d \times \Theta\right) \to \mathbb{R}$ is a random field with a covariance function $C_H : \left(\mathbb{R}^d \times \mathbb{R}^d\right) \to \mathbb{R}$ defined in a space $D \in \mathbb{R}^d$. Since the covariance function is finite, symmetric and positive definite it can be represented by a spectral decomposition. We refer to the books by Ghanem and Spanos [70] and Papoulis and Pillai [71] for detailed introduction on Karhunen–Loève expansion. Using this spectral decomposition, the random process $H(\mathrm{r}, \theta)$ can be expressed in a generalized Fourier type of series as

$$H(\mathrm{r}, \theta) = H_0(\mathrm{r}) + \sum_{j=1}^{\infty} \sqrt{\lambda_j}\xi_j(\theta)\varphi_j(\mathrm{r}) \tag{13}$$

where $\xi_j(\theta)$ are uncorrelated random variables, λ_j and $\varphi_j(\mathrm{r})$ are eigenvalues and eigenfunctions satisfying the integral equation

$$\int_D C_H(\mathrm{r}_1, \mathrm{r}_2)\varphi_j(\mathrm{r}_1)\mathrm{d}\mathrm{r}_1 = \lambda_j\varphi_j(\mathrm{r}_2), \quad \forall\ j = 1, 2, \ldots \tag{14}$$

These associated eigenvalues and eigenfunctions will be used to obtain the boundary or connection stiffness and damping matrices. In fact, there are many kinds of correlation function models of random fields, for example, exponential type and squared exponential type. Gaussian random fields with exponentially decaying autocorrelation function are considered in this paper. For all practical purposes, The series in Eq. (13) can be ordered in a decreasing series so that it can be truncated using a finite number of terms with the desired accuracy. The number of terms could be selected based on the 'amount of information' to be retained.

Suppose that the boundary displacement $\boldsymbol{d}_b(\mathrm{r}, \omega)$ and force $\boldsymbol{f}_b(\mathrm{r}, \omega)$ is described by boundary shape function $\mathrm{N}(\mathrm{r}) \in \mathbb{C}^n$($n$ is the number of the nodal Dofs) and the associated generalized boundary nodal displacements $\widehat{\boldsymbol{d}}_b(\omega) \in \mathbb{C}^n$ and force $\widehat{\boldsymbol{f}}_b(\omega) \in \mathbb{C}^n$ as

$$\boldsymbol{d}_b(\mathrm{r}, \omega) = \mathrm{N}^{\mathrm{T}}(\mathrm{r})\widehat{\boldsymbol{d}}_b(\omega) \tag{15}$$

$$\boldsymbol{f}_b(\mathrm{r}, \omega) = \mathrm{N}^{\mathrm{T}}(\mathrm{r})\widehat{\boldsymbol{f}}_b(\omega) \tag{16}$$

Extending the weak-form of finite element approach to the complex domain, the $n \times n$ stochastic spectral stiffness matrix $\boldsymbol{H}_b(\mathrm{r}, \theta)$ ($\boldsymbol{H}_b(\mathrm{r}, \theta)$ can stand for stochastic boundary stiffness matrix $\boldsymbol{K}_b(\mathrm{r}, \theta)$ and stochastic boundary damping matrix $\boldsymbol{C}_b(\mathrm{r}, \theta)$) can be obtained by combining the boundary shape function $\mathrm{N}(\mathrm{r})$ as

$$\boldsymbol{H}_b(\mathrm{r}, \theta) = \int_{D_b} h_b(\mathrm{r}, \theta)\mathrm{N}(\mathrm{r})\mathrm{N}^{\mathrm{T}}(\mathrm{r})\mathrm{d}\mathrm{r} \tag{17}$$

where $(\bullet)^{\mathrm{T}}$ denotes matrix transpose, $h_b(\mathrm{r}, \theta) : \left(\mathbb{R}^d \times \Theta\right) \to \mathbb{R}$ is the random distributed parameter. The random field $h_b(\mathrm{r}, \theta)$ is expanded using the Karhunen–Loève expansion of Eq. (13). Using sufficient number of terms M_H, the stochastic spectral stiffness matrix can be expanded in a spectral series as

$$\boldsymbol{H}_b(\mathrm{r}, \theta) = \boldsymbol{H}_{0b}(\mathrm{r}) + \sum_{j=1}^{M_{\mathrm{H}}} \xi_{\mathrm{H}_j}(\theta)\boldsymbol{H}_{jb}(\mathrm{r}) \tag{18}$$

Here the deterministic spectral stiffness matrices can be obtained as

$$\boldsymbol{H}_{0b}(\mathrm{r}) = \int_{D_b} h_{b_0}(\mathrm{r})\mathrm{N}(\mathrm{r})\mathrm{N}^{\mathrm{T}}(\mathrm{r})\mathrm{d}\mathrm{r} \tag{19}$$

$$\boldsymbol{H}_{jb}(\mathrm{r}) = \sqrt{\lambda_{\mathrm{H}_j}} \int_{D_b} \varphi_{\mathrm{H}_j}(\mathrm{r})\mathrm{N}(\mathrm{r})\mathrm{N}^{\mathrm{T}}(\mathrm{r})\mathrm{d}\mathrm{r} \quad \forall j = 1, 2, \ldots, M_{\mathrm{H}} \tag{20}$$

where λ_{H_j} and $\varphi_{\mathrm{H}_j}(\mathrm{r})$ are eigenvalues and eigenfunctions. In this manner, the stochastic boundary or connection spectral dynamic stiffness $\boldsymbol{G}_K(\mathrm{r}, \theta)$ and damping $\boldsymbol{G}_C(\mathrm{r}, \theta)$ matrix can be obtained. For notational convenience, the $\boldsymbol{G}_K(\mathrm{r}, \theta)$ and $\boldsymbol{G}_C(\mathrm{r}, \theta)$ can be expressed in a unified form as

$$\boldsymbol{G}(\mathrm{r}, \theta) = \boldsymbol{G}_0(\mathrm{r}) + \sum_{j=1}^{M_{\mathrm{H}}} \xi_j(\theta)\boldsymbol{G}_j(\mathrm{r}) \tag{21}$$

In this equation $\boldsymbol{G}_0$ and $\boldsymbol{G}_j \to \mathbb{C}^{N \times N}$ are stochastic symmetric matrices. N is the dynamic degrees of freedom. In the next section, the derivation of stochastic spectral stiffness matrix using modified Fourier series (MFs) as boundary or connection shape function $\mathrm{N}(\mathrm{r})$ will be introduced in detail.

3.2. SSDS formulation for spatially-varying viscoelastic BCs and CCs with uncertainties

Next, the MFs are used to develop the stochastic spectral dynamic stiffness matrix of uncertain boundary or connection spatial function $G(\mathrm{r})$ following the steps in Section 3.1. In this paper, Gaussian random fields with an exponentially decaying autocorrelation function were considered. The correlation function can be expressed as

$$R(\mathrm{r}_1,\mathrm{r}_2)=e^{-|\mathrm{r}_1-\mathrm{r}_2|c} \tag{22}$$

where the c is inversely proportional to the correlation length. The stochastic dimensionless spatial function $G(\mathrm{r},\theta)$ can be expressed as

$$G(\mathrm{r},\theta)=G_0(\mathrm{r})+\sum_{i=1}^{\infty}\left(\sqrt{\lambda_i}\xi_i(\theta)\varphi_i(\mathrm{r})+\sqrt{\lambda_{i^*}}\xi_{i^*}(\theta)\varphi_{i^*}(\mathrm{r})\right) \tag{23}$$

where $\xi_i(\theta)$ and $\xi_{i^*}(\theta)$ are uncorrelated random coefficients, λ_i, λ_{i^*} and $\varphi_i(\mathrm{r})$, $\varphi_{i^*}(\mathrm{r})$ are eigenvalues and eigenfunctions. Since parameter is assumed to be a Gaussian random field, without any loss of generality we assumed the mean to be zero, thus the eigenvalues and eigenfunctions in the K-L expansion for odd i are given by

$$\lambda_i=\frac{2c}{\omega_i^2+c^2}\qquad \varphi_i(\mathrm{r})=\frac{\cos\left(\omega_i\mathrm{r}\right)}{\sqrt{L+\frac{\sin(2\omega_i L)}{2\omega_i}}}\qquad \text{where}\quad \tan(\omega_i L)=\frac{c}{\omega_i}, \tag{24}$$

and for even i

$$\lambda_{i^*}=\frac{2c}{\omega_i^{*2}+c^2}\qquad \varphi_{i^*}(\mathrm{r})=\frac{\sin\left(\omega_i^*\mathrm{r}\right)}{\sqrt{L-\frac{\sin(2\omega_i^* L)}{2\omega_i^*}}}\qquad \text{where}\quad \tan(\omega_i^* L)=\frac{\omega_i^*}{-c}. \tag{25}$$

These eigenvalues and eigenfunctions can be used to obtain the stochastic stiffness and damping matrices. The infinite series in Eq. (23) needs to be truncated at a finite number of terms N, which could be determined by the required description accuracy of the random fields. If more truncate terms are included, the random fields can be described more accurately, and vice versa.

Since in the spectral dynamic stiffness method, considering n number of terms in the KL expansion to the $G(\mathrm{r},\theta)$, the global spectral boundary distribution matrix in Eq. (21) can be expressed as

$$\boldsymbol{G}(\mathrm{r},\theta)=\boldsymbol{G}_0(\mathrm{r})+\sum_{i=1}^{n/2}\left(\sqrt{\lambda_i}\xi_i(\theta)\widetilde{\boldsymbol{G}}^{i}(\mathrm{r})+\sqrt{\lambda_{i^*}}\xi_{i^*}(\theta)\widetilde{\boldsymbol{G}}^{i^*}(\mathrm{r})\right) \tag{26}$$

where

$$\boldsymbol{G}_{0tl}=\frac{1}{\sqrt{\zeta_{tr}\zeta_{ls}}L}\int_{-L}^{L}\left[G_0(\mathrm{r})\mathcal{T}_l(\gamma_{ls}\mathrm{r})\mathcal{T}_t(\gamma_{tr}\mathrm{r})\right]\mathrm{d}\mathrm{r} \tag{27}$$

$$\widetilde{\boldsymbol{G}}_{tl}^{i}=\frac{1}{\sqrt{\zeta_{tr}\zeta_{ls}}L}\int_{-L}^{L}\left[\varphi_i(\mathrm{r})\mathcal{T}_l(\gamma_{ls}\mathrm{r})\mathcal{T}_t(\gamma_{tr}\mathrm{r})\right]\mathrm{d}\mathrm{r} \tag{28}$$

$$\widetilde{\boldsymbol{G}}_{tl}^{i^*}=\frac{1}{\sqrt{\zeta_{tr}\zeta_{ls}}L}\int_{-L}^{L}\left[\varphi_{i^*}(\mathrm{r})\mathcal{T}_l(\gamma_{ls}\mathrm{r})\mathcal{T}_t(\gamma_{tr}\mathrm{r})\right]\mathrm{d}\mathrm{r} \tag{29}$$

where $\mathcal{T}_l(\gamma_{ls}\mathrm{r})$ is the corresponding modified Fourier basis function which is described in the Appendix A. The deterministic SDS matrix $\boldsymbol{G}_{0tl}$ has been obtained [66], and stochastic SDS matrix $\widetilde{\boldsymbol{G}}_{tl}^{i}$, $\widetilde{\boldsymbol{G}}_{tl}^{i^*}$ can be obtained by using the integrals of Eqs. (28)–(29). For the sake of notational convenience, some notations are introduced. If S terms are adopted in the series solution ($s\in[0,S-1]$), then $\mathrm{diag}(\cdot)_{S^0}$ is used to denote a diagonal matrix with the 's' in expression '$\cdot$' taking $s\in[0,S-1]$, also $\mathrm{diag}(\cdot)_{S^1}$ with '$\cdot$' taking $s\in[1,S-1]$. Similarly, $[\cdot]_{0,S^1}$ stands for a row vector with '$\cdot$' taking $r=0$ and $s\in[1,S-1]$; $[\cdot]_{S^1,0}$ represents a column vector with '$\cdot$' taking $r\in[1,S-1]$, $s=0$; $[\cdot]_{S^1,S^1}$ denotes a matrix with '$\cdot$' taking $r\in[1,S-1]$, $s\in[1,S-1]$ and so on. By using the expression of the eigenfunction for the odd values of i, as in Eq. (24), for $\widetilde{\boldsymbol{G}}_{tl}^{i}$, $\widetilde{\boldsymbol{G}}_{01}^{i}=\widetilde{\boldsymbol{G}}_{10}^{i}=\boldsymbol{0}$

$$\left[\widetilde{\boldsymbol{G}}_{00}^{i}\right]=F_5\begin{bmatrix}\frac{F_3}{F_1} & \left[\frac{(-1)^s\sqrt{2}F_1F_3}{F_1^2-\pi^2s^2}\right]_{1,S-1}\\ \left[\frac{(-1)^r\sqrt{2}F_1F_3}{F_1^2-\pi^2r^2}\right]_{S-1,1} & \left[\frac{2(-1)^{r+s}F_1\left(F_1^2-\pi^2\left(r^2+s^2\right)\right)F_3}{(F_1+\Sigma_1)(F_1-\Sigma_1)(F_1-\Sigma_2)(F_1+\Sigma_2)}\right]_{S-1,S-1}\end{bmatrix}, \tag{30}$$

except for the diagonal terms

$$\widetilde{\boldsymbol{G}}_{00}^{i}(r,s)=F_5\left[\frac{2\left(F_1^2-2\pi^2s^2\right)F_3}{\omega_i^3L^3-4F_1\pi^2s^2}\right] \tag{31}$$

for $r=s\in[0,S-1]$.

$$\left[\widetilde{\boldsymbol{G}}_{11}^{i}\right]=F_5\left[\left[\frac{(-1)^{1+r+s}F_1\left(-2F_1^2+\pi^2(1+2r(1+r)+2s(1+s))\right)F_3}{(F_1+\Sigma_1)(F_1-\Sigma_1)(F_1-\Sigma_2-\pi)(F_1+\pi+\Sigma_1)}\right]_{S,S}\right], \tag{32}$$

except for the diagonal terms

$$\widetilde{\boldsymbol{G}}_{11}^{i} = F_5\left[-\frac{\left(-2F_1^2+(\pi+2\pi s)^2\right)F_3}{F_1(F_1+\pi(1+2s))(F_1-\pi(1+2s))}\right] \tag{33}$$

for $r = s \in [0, S]$.

In a similar manner, by using the expression of the eigenfunction for the even values of i, as in Eq. (25), for $\widetilde{\boldsymbol{G}}_{tl}^{i^*}$, $\widetilde{\boldsymbol{G}}_{00}^{i^*} = \widetilde{\boldsymbol{G}}_{11}^{i^*} = \boldsymbol{0}$

$$\widetilde{\boldsymbol{G}}_{10}^{i^*T} = \widetilde{\boldsymbol{G}}_{01}^{i^*} = F_6\begin{bmatrix} \left[\frac{4(-1)^s\sqrt{2}F_2F_4}{(-2F_2+\pi+2\pi s)(2F_2+\pi+2\pi s)}\right]_{1,S} \\ \left[\frac{8(-1)^{r+s}F_2\left(-4F_2^2+\pi^2\left(4r^2+(1+2s)^2\right)\right)F_4}{(2F_2-\pi+2\Sigma_1)(2F_2+\pi-2\Sigma_1)(2F_2+\pi+2\Sigma_2)(2F_2-\pi-2\Sigma_2)}\right]_{S-1,S} \end{bmatrix}, \tag{34}$$

except for the diagonal terms

$$\widetilde{\boldsymbol{G}}_{10}^{i^*} = \widetilde{\boldsymbol{G}}_{01}^{i^*} = F_6\left[\frac{8F_2\left(-4F_2^2+\pi^2\left(1+4s+8s^2\right)\right)F_4}{\left(-4F_2^2+\pi^2\right)(-2F_2+\pi+4\pi s)(2F_2+\pi+4\pi s)}\right] \tag{35}$$

for $r = s \in [0, S]$. where

$$F_1 = \omega_i L, \qquad F_2 = \omega_i^* L, \qquad F_3 = \sin(\omega_i L)$$
$$F_4 = \cos(\omega_i^* L), \qquad F_5 = \frac{1}{\sqrt{L+\frac{\sin(2\omega_i L)}{2\omega_i}}}, \qquad F_6 = \frac{1}{\sqrt{L-\frac{\sin(2\omega_i^* L)}{2\omega_i^*}}}$$
$$\Sigma_1 = \pi(r-s), \qquad \Sigma_2 = \pi(r+s)$$

After obtaining the deterministic part and stochastic part of the SDS matrices, the SDS matrix $\boldsymbol{G}(\mathrm{r},\theta)$ can be derived by Eq. (26). Then, by assembling $\boldsymbol{G}(\mathrm{r},\theta)$ in the way of Sections 2.2.1 and 2.2.2, the whole SSDS matrix $\boldsymbol{K}^{final}$ of plate-like structure with uncertain BCs or CCs can be obtained in a similar form to Eqs. (8) and (12). For viscoelastic supports with uncertainties, we have

$$\boldsymbol{K}_{ii}^{final} = \boldsymbol{K}_{ii} + \mu_K \boldsymbol{G}_K(\mathrm{r},\theta) + \mathrm{i}\mu_C \boldsymbol{G}_C(\mathrm{r},\theta)\,. \tag{36}$$

For viscoelastic coupling constrains with uncertainties, we have

$$\begin{aligned} \boldsymbol{K}_{ii}^{final} &= \boldsymbol{K}_{ii} + \mu_K \boldsymbol{G}_K(\mathrm{r},\theta) + \mathrm{i}\mu_C \boldsymbol{G}_C(\mathrm{r},\theta)\,, \\ \boldsymbol{K}_{jj}^{final} &= \boldsymbol{K}_{jj} + \mu_K \boldsymbol{G}_K(\mathrm{r},\theta) + \mathrm{i}\mu_C \boldsymbol{G}_C(\mathrm{r},\theta)\,, \\ \boldsymbol{K}_{ij}^{final} &= \boldsymbol{K}_{ij} - [\mu_K \boldsymbol{G}_K(\mathrm{r},\theta) + \mathrm{i}\mu_C \boldsymbol{G}_C(\mathrm{r},\theta)]\,, \\ \boldsymbol{K}_{ji}^{final} &= \boldsymbol{K}_{ji} - [\mu_K \boldsymbol{G}_K(\mathrm{r},\theta) + \mathrm{i}\mu_C \boldsymbol{G}_C(\mathrm{r},\theta)]\,. \end{aligned} \tag{37}$$

Finally, arbitrary uncertain spatially-varying viscoelastic supports and coupling constrains are analytically modeled.

4. Stochastic eigenvalue analysis based on the extended Wittrick–Williams algorithm

Then the proposed stochastic spectral dynamic stiffness model can be used for stochastic eigenvalue analysis of plates with uncertain boundary or connection conditions. The extended Wittrick–Williams (WW) algorithm [64] is applied to the SSDS formulation of final structures to obtain any required natural frequencies with any desired accuracy. This algorithm ensures that no eigenvalue is missed by monitoring the Sturm sequence of the ensuring matrix. The extended WW algorithm [64] is an improvement on the well-known WW [72], according to the WW algorithm, the number of eigenvalues between 0 and a trial frequency ω^* (mode count J) of the final structure is

$$J = J_0 + s\left\{\boldsymbol{K}^{final}\right\} \tag{38}$$

where $s\left\{\boldsymbol{K}^{final}\right\}$ is the number of negative elements on the leading diagonal of $\boldsymbol{K}^{\Delta}$, and $\boldsymbol{K}^{\Delta}$ is the upper triangular matrix obtained by applying the usual form of Gauss elimination to $\boldsymbol{K}^{final}$, and J_0 is the number of natural frequencies of the structure still lying between $\omega = 0$ and $\omega = \omega^*$ when the displacement components to which $\boldsymbol{K}^{final}$ corresponds are all zeros. By Section 3.2, the $\boldsymbol{K}^{final}$ matrix can be obtained. J_0 can be computed in a concise way by using the extended WW algorithm [64]. Once the final $\boldsymbol{K}^{final}$ of different random samples are given, their corresponding eigensolutions will be computed. This algorithm can be used for stochastic eigenvalue analysis of plate assembly subject to uncertain elastic BCs or CCs.

5. Stochastic dynamic response analysis

For stochastic dynamic response analysis, if the amplitude of a harmonic excitation on the ith boundary is described by $F_i^b(\mathrm{r})$, then the spectral representation of this excitation can be derived by substituting $F_i^b(\mathrm{r})$ into Eq. (A.5a) leading to the associated modified Fourier series coefficients, which can be written in a vector form $\boldsymbol{f}_i$. The analytical expressions for $\boldsymbol{f}_i$ corresponding to

several functions $F_i^b(\mathrm{r})$ are given in Appendix B. Once all boundary excitations $\boldsymbol{f}_i$ are written in modified Fourier coefficients vector form, the overall generalized force for the whole built-up structure can be given by $\boldsymbol{f}^{final}$, and we have

$$\boldsymbol{K}^{final}\boldsymbol{d}^{final} = \boldsymbol{f}^{final} \tag{39}$$

where $\boldsymbol{K}^{final}$ is the global stochastic spectral dynamic stiffness matrix of plate built-up structure, $\boldsymbol{d}^{final}$ is the response of the overall generalized boundary displacement vector in the form of the modified Fourier coefficients of along all boundaries of the plate assembly. In the subsequent sections we present two strategies to compute the response of generalized displacement vector $\boldsymbol{d}^{final}$. The first approach is the direct matrix inversion method, whereas the second approach is an improved response analysis method based on domain decomposition method. The two approaches are detailed as below.

5.1. Response analysis based on the stochastic spectral dynamic stiffness matrix by using direct matrix inversion

The response in the form of generalized displacements of $\boldsymbol{d}^{final}$ can be obtained by directly inversing $\boldsymbol{K}^{final}$ matrix and multiplied to the excitation in the form of $\boldsymbol{f}^{final}$ based on Eq. (39). By matrix operations, we have

$$[\boldsymbol{d}^{final}] = [\boldsymbol{K}^{final}]^{-1}[\boldsymbol{f}^{final}] \tag{40}$$

where $\boldsymbol{d}^{final}$ includes both deterministic part and stochastic part. For this method, there is no need to perform additional operations on $\boldsymbol{K}^{final}$ in the process of matrix inversion, and the inverse of $\boldsymbol{K}^{final}$ is directly performed by Eq. (40) to obtain $\boldsymbol{d}^{final}$. But the global stochastic spectral stiffness matrix $\boldsymbol{K}^{final}$ needs to be calculated repeatedly with the change of random samples, which means that each case in the uncertain boundary or connection conditions corresponds to a kind of $\boldsymbol{K}^{final}$ and $\boldsymbol{d}^{final}$, and $\boldsymbol{f}^{final}$ remains unchanged.

5.2. Improved response analysis based on the stochastic spectral dynamic stiffness matrix by using domain decomposition

Although the direct matrix inverse operation is simple, the computational cost increases as the size of $\boldsymbol{K}^{final}$ matrix increases. Moreover, every random sample needs to carry out an overall matrix inverse, which has negative impacts on the computational cost and accuracy. In this paper, a matrix operation method is designed to improve the computational efficiency. Eq. (39) can be written as follows:

$$\begin{bmatrix} \boldsymbol{f}_D \\ \boldsymbol{f}_S \end{bmatrix} = \begin{bmatrix} \boldsymbol{K}_{DD} & \boldsymbol{K}_{DS} \\ \boldsymbol{K}_{SD} & \boldsymbol{K}_{SS} \end{bmatrix} \begin{bmatrix} \boldsymbol{d}_D \\ \boldsymbol{d}_S \end{bmatrix} \tag{41}$$

where $\boldsymbol{f}_D$ ($\boldsymbol{d}_D$) and $\boldsymbol{f}_S$ ($\boldsymbol{d}_S$) represent the modified Fourier coefficients of forces (displacements) corresponding to deterministic boundaries and stochastic boundaries of the plate assemblies, respectively. The final spectral dynamic stiffness matrix $\boldsymbol{K}^{final}$ is divided into four blocks, where $\boldsymbol{K}_{SS}$ represents the spectral dynamic stiffness matrix of the boundaries subject to uncertain BCs or CCs in the plate assemblies and the other three blocks ($\boldsymbol{K}_{DD}$, $\boldsymbol{K}_{DS}$, $\boldsymbol{K}_{SD}$) are the deterministic SDS matrices. In particular, $\boldsymbol{K}_{SS}$ can be expressed in the summation of deterministic part $\boldsymbol{K}_{SSD}$ and stochastic part $\Delta\boldsymbol{K}$.

$$\boldsymbol{K}_{SS} = \boldsymbol{K}_{SSD} + \Delta\boldsymbol{K} \tag{42}$$

In the final spectral dynamic stiffness matrix, only the stochastic part $\Delta\boldsymbol{K}$ needs to be evaluated cyclically within random samples in the stochastic dynamic response analysis. The other three deterministic blocks $\boldsymbol{K}^{final}$, $\boldsymbol{K}_{DD}$, $\boldsymbol{K}_{DS}$, $\boldsymbol{K}_{SD}$ only need to be computed once for all. This not only reduces the size of the matrix to be calculated, but also reduces the risk of numerical instability in the matrix operation. Therefore, this improvement on response analysis is more computational efficient and reliable than the direct matrix inversion method of Eq. (40). The detailed derivation is given as follows. According to Eq. (41), we have

$$\boldsymbol{d}_D = \boldsymbol{K}_{DD}^{-1}\left(\boldsymbol{f}_D - \boldsymbol{K}_{DS}\boldsymbol{d}_S\right) \tag{43}$$

Similarly, the equation related to $\boldsymbol{f}_S$ combined with Eq. (43) can be expressed as

$$\begin{aligned} \boldsymbol{f}_S &= \boldsymbol{K}_{SD}\boldsymbol{d}_D + \boldsymbol{K}_{SS}\boldsymbol{d}_S \\ &= \boldsymbol{K}_{SD}\boldsymbol{K}_{DD}^{-1}\left(\boldsymbol{f}_D - \boldsymbol{K}_{DS}\boldsymbol{d}_S\right) + \boldsymbol{K}_{SS}\boldsymbol{d}_S \\ &= \boldsymbol{K}_{SD}\boldsymbol{K}_{DD}^{-1}\boldsymbol{f}_D - \boldsymbol{K}_{SD}\boldsymbol{K}_{DD}^{-1}\boldsymbol{K}_{DS}\boldsymbol{d}_S + \boldsymbol{K}_{SS}\boldsymbol{d}_S \end{aligned} \tag{44}$$

Next, according to Eq. (44), $\boldsymbol{d}_S$ can be expressed as

$$\begin{aligned} \boldsymbol{d}_S &= \left(\boldsymbol{K}_{SD}\boldsymbol{K}_{DD}^{-1}\boldsymbol{f}_D - \boldsymbol{f}_S\right)\left(\boldsymbol{K}_{SD}\boldsymbol{K}_{DD}^{-1}\boldsymbol{K}_{DS} - \boldsymbol{K}_{SS}\right)^{-1} \\ &= \left(\hat{\boldsymbol{K}}\boldsymbol{f}_D - \boldsymbol{f}_S\right)\left(\hat{\boldsymbol{K}}\boldsymbol{K}_{DS} - \boldsymbol{K}_{SSD} - \Delta\boldsymbol{K}\right)^{-1} \end{aligned} \tag{45}$$

where

$$\hat{\boldsymbol{K}} = \boldsymbol{K}_{SD}\boldsymbol{K}_{DD}^{-1} \tag{46}$$

Finally, combining with Eqs. (43) to (45), the response of generalized displacement vector $\boldsymbol{d}^{final}$ can be expressed as

$$\boldsymbol{d}^{final} = \begin{bmatrix} \boldsymbol{d}_D \\ \boldsymbol{d}_S \end{bmatrix} \tag{47}$$

For the calculation of Eq. (47), only $\boldsymbol{d}_S$ will be calculated in a cyclic manner within random samples, while $\boldsymbol{d}_D$ will not be repeatedly calculated within random samples, which again reduces the computational cost.

Next, it is possible to recover the stochastic dynamic response of the whole plate assembly along the plate nodal boundaries as well as all domain points. By substituting the generalized displacements $\boldsymbol{d}^{final}$ on the nodal boundaries into Eq. (48) and taking inverse modified Fourier transformation, the dynamic response $U^b(\mathrm{r})$ at any point along the nodal boundaries can be obtained as follows.

$$U^b(\mathrm{r}) = \sum_{\substack{s\in\mathbb{N}\\ l\in\{0,1\}}} \boldsymbol{d}^{final} \frac{\mathcal{T}_l(\gamma_{ls}\mathrm{r})}{\sqrt{\zeta_{ls}L}} \tag{48}$$

Further, once we obtain the generalized displacements $\boldsymbol{d}^{final}$, the nodal displacement vector for all domain points can be easily developed. The general solutions of Eq. (1) now can be partitioned into a sum of four component solutions [64,67] in each of which the function $W^{kj}(x,y)$ is either even or odd. We have

$$W(x,y) = \sum_{k,j\in\{0,1\}} W^{kj}(x,y) = W^{00} + W^{01} + W^{10} + W^{11} \tag{49}$$

$$\begin{aligned} W^{kj}(x,y) = &\sum_{m\in\mathbb{N}} \left[A_{1km}\mathcal{H}_j\left(p_{1km}y\right) + A_{2km}\mathcal{H}_j\left(p_{2km}y\right)\right]\mathcal{T}_k\left(\alpha_{km}x\right) \\ &+ \sum_{n\in\mathbb{N}} \left[B_{1jn}\mathcal{H}_k\left(q_{1jn}x\right) + B_{2jn}\mathcal{H}_k\left(q_{2jn}x\right)\right]\mathcal{T}_j\left(\beta_{jn}y\right) \end{aligned} \tag{50}$$

where the indices k (related to x direction) and j (related to y direction), taking in turn with values either '0' or '1', represent either symmetric or antisymmetric functions in the related directions. $\mathcal{T}$ stands for trigonometric functions defined in Eq. (A.3) and $\mathcal{H}$ represents hyperbolic functions [64,67]. A_{1km}, A_{2km}, B_{1jn}, B_{2jn} are the coefficients associated with $\boldsymbol{d}^{final}$ [64,67]. According to Eq. (50), we can obtain the response of each plate element at some arbitrary location (x_0, y_0). Finally, the stochastic dynamic responses of the whole plate assembly can be obtained.

6. Results and discussions

After illustrating the theoretical framework of the proposed methodology, the above solution technique have been implemented in a Matlab code. It is now applied to compute eigenvalues and dynamic responses of single plates and plate assemblies under uncertain boundary conditions and connection conditions. In Section 6.1, we consider the elastic constraints stiffness as Gaussian random fields and discuss the statistics of the eigenvalues of undamped free vibration of single plate through the direct Monte Carlo simulation. In Section 6.2, the stochastic dynamic response of a single plate under stochastic spring stiffness and damping, and plate assemblies under stochastic viscoelastic coupling stiffness and damping are obtained using the developed stochastic spectral dynamic stiffness formulas (36)–(37) respectively.

6.1. Stochastic eigenvalue analysis with uncertain elastic support

This section takes a single plate structure as an example. The mean material properties of plate are considered density ρ_0 = 2700 kg/m^3, and modulus of elasticity E_0 = 69 GPa. Poisson's ratio μ = 0.3. The thickness h = 0.001 m. The length and width of the plate are 0.5 m and 1 m respectively. The boundary condition of the plate is four sides are simply supported and torsion of three sides are stochastic elastic supported. We consider the elastic constraints stiffness as Gaussian random fields and the mean of elastic constraint stiffness $k_\phi = k_{\phi 0}G(r)$, $k_{\phi 0} = 6.3D/(2a)$, D is the bending rigidity of the plate, $G(r) = [1-(r/L)^2]/4$. The 'strength parameters' ϵ is assumed to be 0.2. The correlation length of the random fields describing k_ϕ are assumed to be $L/2$.

The accuracy and efficiency of the spectral dynamic stiffness method for solving the dynamic characteristics of plate structures with deterministic boundary conditions have been proved in previous studies [66], so the stochastic dynamic characteristics of plate structures are straightforwardly analyzed in this paper. The natural frequencies of plates with stochastic elastic support are computed directly by the enhanced Wittrick–Williams algorithm [66]. Through Monte Carlo simulation, a total of 1000 samples are computed to obtain the statistics and the probability density functions of the eigenvalues.

The statistical scatter of the first six eigenvalues by using SSDSM are shown in Fig. 3. Solid lines represent the eigenvalues for the corresponding deterministic plate model with average parameters, whose values are $\overline{\lambda}_1$ = 13.878 Hz, $\overline{\lambda}_2$ = 20.476 Hz, $\overline{\lambda}_3$ = 32.232 Hz $\overline{\lambda}_4$ = 41.119 Hz, $\overline{\lambda}_5$ = 48.923 Hz, $\overline{\lambda}_6$ = 49.773 Hz. While each random scatter denotes the eigenvalue of the corresponding random parameters with the given sample. It can be seen that the first two eigenvalues are well separated and little statistical overlap exists between them. In addition, the scattering degree of the fourth eigenvalue is larger than that of the other eigenvalues, which indicates that the uncertainty of elastic support constraints influences the fourth eigenvalue most. The scattering degrees of other eigenvalues are similar.

The probability density distribution curves from the MSC results for the first six eigenvalues calculated by extended WW algorithm are shown in Fig. 4. At the same time, the curves drawn using three probability distribution methods [42] (Kernel density estimation distribution, χ^2 distribution, Truncated Gaussian distribution) are also shown in the figure. It can be seen that those methods agree well with the Monte Carlo simulation results. And there is no overlap between the modes, which is in good agreement with the observation in Fig. 3. The proposed SSDSM method can be used to analyze stochastic eigenvalues of plates subject to arbitrary spatially-varying elastic boundary conditions with uncertainties.

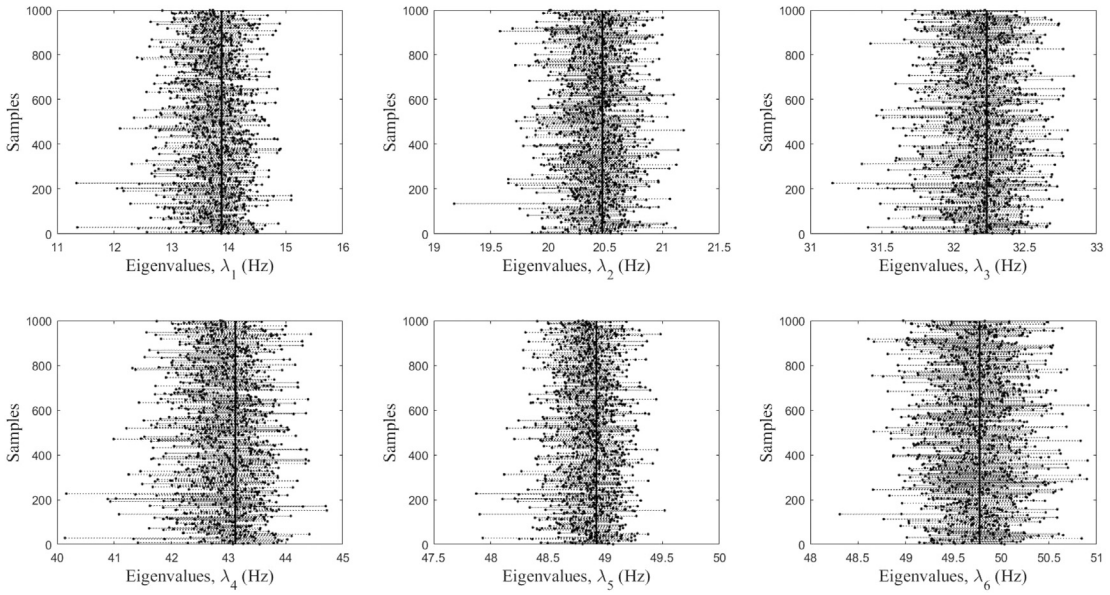

Fig. 3. Statistical scatter of the first six eigenvalues of the single plate with uncertain elastic support by using SSDSM. The six vertical continuous lines represent the deterministic eigenvalues for the first six eigenmodes.

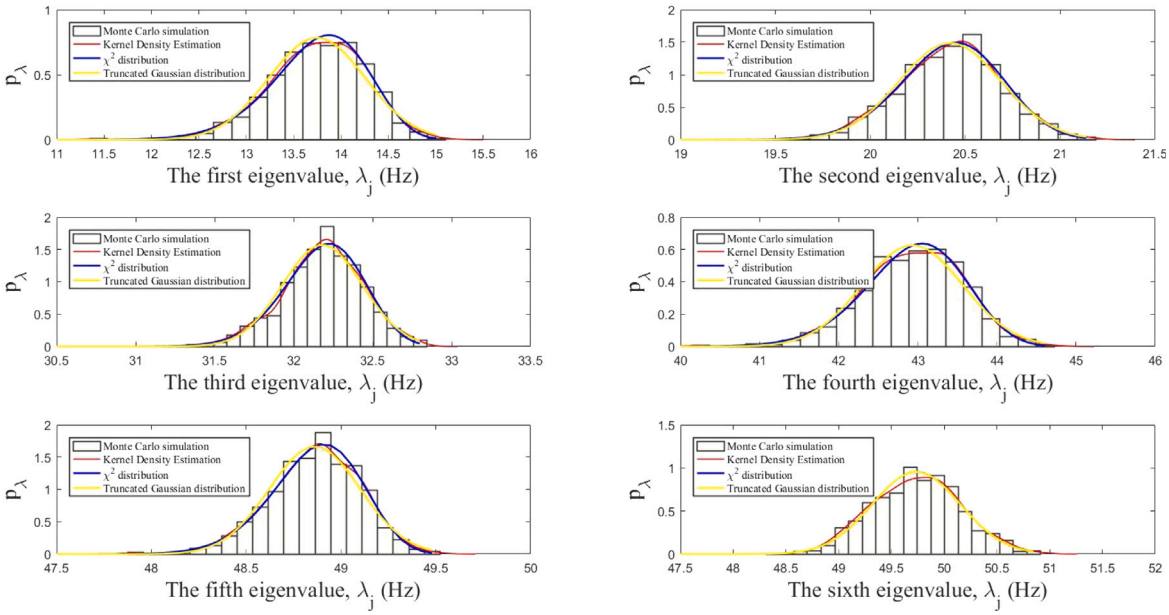

Fig. 4. Probability density functions of the first six eigenvalues of the single plate with uncertain elastic support by using SSDSM.

6.2. Stochastic dynamic response analysis of plates with uncertain boundary or connection conditions

In this subsection, the dynamic response analysis of a plate with uncertain viscoelastic supports and coupling constraint is considered. Section 6.2.1 uses the proposed method to compute the response curve and displacement response field of the plate with uncertain elastic supports, and the high accuracy and efficiency of this method is demonstrated. Section 6.2.2 computes the response curve and displacement response field of the plate with uncertain coupling connection and analyzes the influence of the uncertainty boundary or connection on the dynamic response.

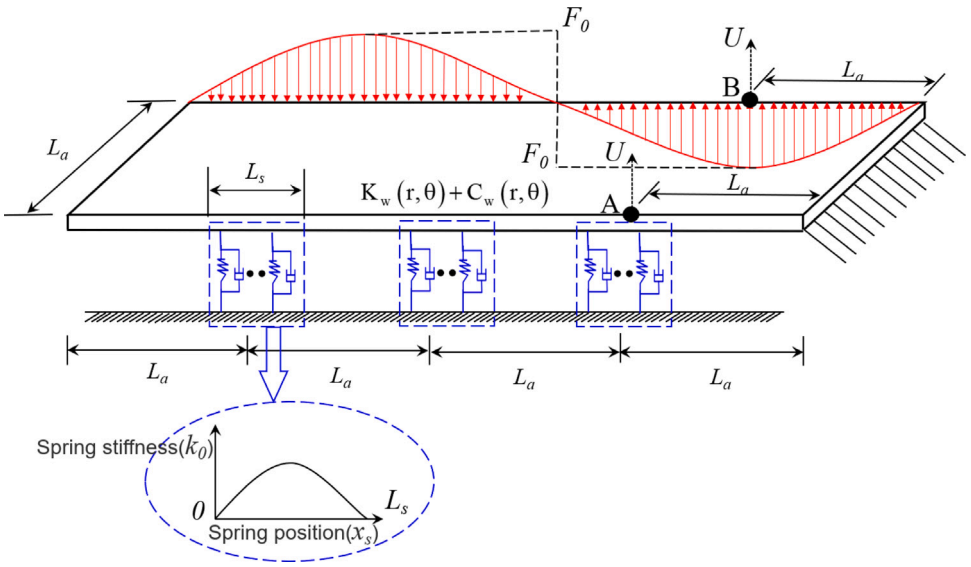

Fig. 5. A rectangular plate with uncertain spatially-varying viscoelastic supports subject to a sine-shape harmonic excitation.

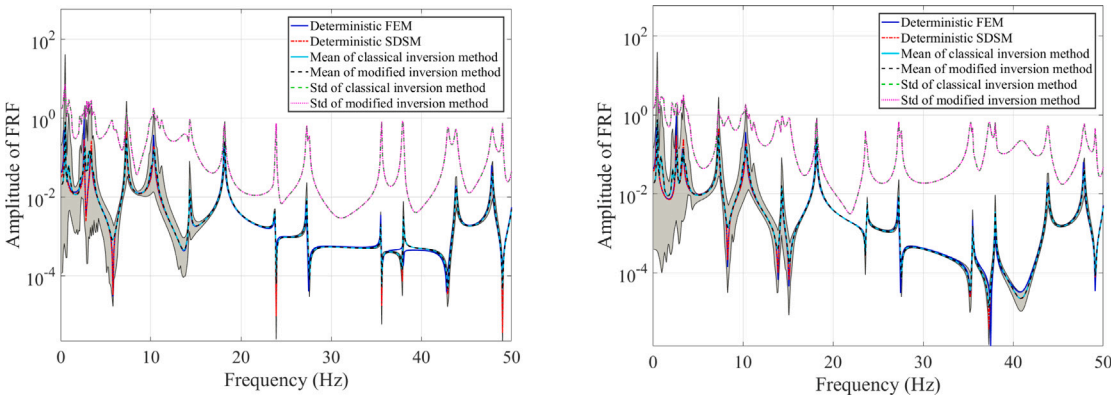

Fig. 6. The absolute value amplitudes of stochastic dynamic responses at point A (left plot) and point B (right plot) shown in Fig. 5 exerted by sine-shaped harmonic excitation. (The gray area represent the responses of the 1000 samples).

6.2.1. *Stochastic dynamic response analysis of single plate with uncertain viscoelastic supports*

The boundary conditions and excitation of the plate are shown in Fig. 5. In this figure, the right side of the plate is clamped and the left side is free. The front side is subject to stochastic spatially-varying translational viscoelastic supports which the mean of the stiffness and damping of the three positions supported presents a sin function distribution, with $k_0 = 1.5(D/(2a)^3)\sin(\frac{\pi x_s}{2L_s})$, $L_s \in \{0, 0.02\}$ and $c_0 = 0.015(D/(2a)^3)\sin(\frac{\pi x_s}{2L_s})$. We consider sin-excitation with $F_0 = 100\sin(\frac{\pi x}{2L_a})$ N/m as the boundary excitation in the back side.

The material properties are density $\rho = 2700$ kg/m^3, Young's modulus $E = 69$ GPa and Poisson's ratio $\nu = 0.3$. The length, width, and height of the plate are $a = 2$ m, $b = 0.5$ m and $h = 0.008$ m respectively. The standard deviations of the random fields for stiffness k and damping c are assumed to be 10% of the mean values of the random fields, so the 'strength parameters' are considered as $\epsilon_k = 0.1$ and $\epsilon_c = 0.1$. The correlation lengths of the random fields for k and c are assumed to be $a/2$.

Following the formulations in Sections Section 5, the response can be readily computed subject to the aforementioned harmonic excitations. The response is computed up from 0 Hz to 50 Hz covering the first fifteen natural modes of the plate. For the dynamic response analysis by SSDSM, the truncation number m, n for the series in Eq. (50) is taken to be 30 after convergence check.

The deterministic response, the mean, and the standard deviation of the absolute value of the stochastic response at point A and point B (shown in Fig. 5) subject to sine-shaped harmonic excitation are shown in Fig. 6. The response curve in the figure includes the determination value of FEM results and SDSM results, the mean of stochastic SDSM results combined with the direct matrix inversion method and the domain decomposition method. To obtain these results, we use a Monte Carlo simulation by generating 1000 samples. In the KL expansion, 18 terms are used for the uncertain viscoelastic supports. The element matrices

Table 1
Displacement and stochastic response field at five frequencies subject to sine-shaped harmonic excitation shown in Fig. 5.

	Deterministic model (1 sample)		Stochastic model (SSDSM) (1000 samples)	
	FEM	SDSM	Direct matrix inversion	Domain decomposition
10 Hz				
20 Hz				
30 Hz				
40 Hz				
50 Hz				

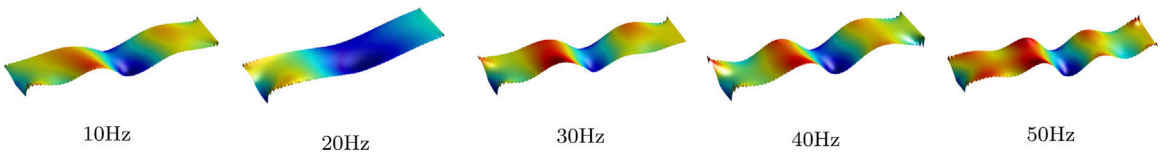

Fig. 7. Standard deviation of displacement response field at five frequencies subject to sine-shaped harmonic excitation shown in Fig. 5 based on the stochastic SDS model.

based on 18 terms are obtained by the formulations derived in Section 3. Some meaningful observations can be made based on Fig. 6. First, the deterministic response obtained by SDSM agrees very well with the finite element results (the mesh size is 400 × 200), while the SDSM results are obtained by using an individual SDS element. For the stochastic response analysis, based on the stochastic SDS model, the mean curve and the standard deviation curve obtained by the direct matrix inversion method and the domain decomposition method are completely coincident, which verifies the accuracy of the latter method. However, there are some discrepancies between the means of responses and the deterministic responses at lower frequencies but almost coincident at high frequencies.

This is expected, since in the lower frequency range, the vibration behavior of plate is more sensitive to the boundary conditions, and therefore large variation occurs when the plate is subject to uncertain BCs. As for the standard deviations of the responses, they are biased by the means and some peaks are reached around the natural frequencies. Similarly, the stochastic dynamic analysis can also be performed for plate assemblies with uncertain boundary or connection conditions.

In order to investigate the displacement response field of the whole structural domain, Table 1 and Fig. 7 show the deterministic, mean and standard deviation (std) of the displacement response field subject to the aforementioned excitation at five different frequencies. Particularly, Table 1 compares the displacement response fields computed by four different methods. It can be found that the mean of the stochastic displacement response field matches well with the deterministic displacement response field obtained by FEM and SDSM. Fig. 7 is the standard deviation of the displacement response field obtained by the stochastic SDS model. As the frequency increases, the standard deviation of displacement response field becomes more complex, as expected.

6.2.2. Stochastic dynamic response analysis of plate systems with uncertain viscoelastic coupling constraints

Next, another problem is investigated by the proposed SSDSM to consider plates with uncertain viscoelastic coupling constraints. Here two isotropic rectangular plates (denoted by plates 1 and 2) are connected by viscoelastic coupling constraints as shown in Fig. 8. The material properties for both plates are: Young's modulus $E = 69$ GPa, Poisson's ratio $\nu = 0.3$ and density $\rho = 2700$ kg/m^3. The two plates have thickness $h_1 = h_2 = 0.008$ m, length $L_a = L_b = 0.8$ m. Except for the edges of the two viscoelastic coupling constraints, one side of each plate is clamped and the rest is free. Both of the translational and rotational coupling stiffnesses are uniformly distributed with the coupling stiffness constants C_w and C_ϕ taking same values: $C_w = 455D/(2a)^3$ and $C_\phi = 16D/(2a)$. In the SDSM implementation, two elements are used for this case. The SDS matrix for the viscoelastic coupling constraints is formulated following the procedure described in Section 2.2.2, which is superposed directly onto that of the two-plate system.

In general, we consider two types of boundary excitations including uniform and sine-shaped with amplitudes of 1N/m and $\sin(\frac{\pi x}{2La})$ N/m respectively, as shown in Fig. 8(a) and 8(b). The deterministic response, the mean and the standard deviation of the absolute value of the response at point A on the free edge as shown in Fig. 8 subject to two types of excitations are shown in Fig. 9. The response curve in the figure includes the determination value of SDSM results and the mean of stochastic SDSM results. To

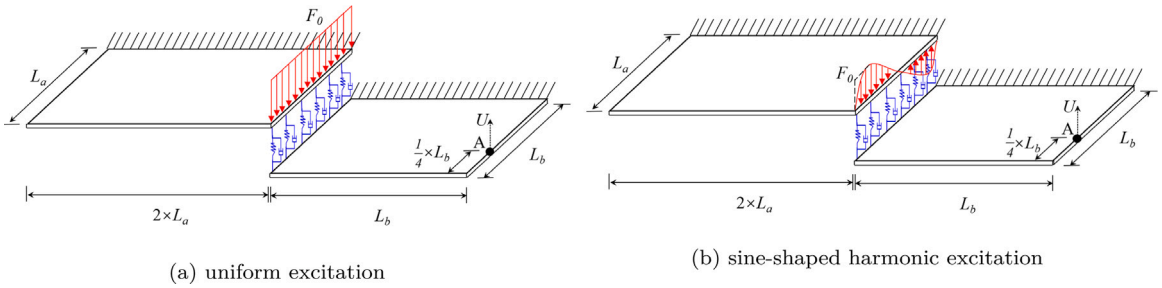

Fig. 8. Two cantilevered plates connected by uncertain viscoelastic coupling constraints subject to two different types of excitation.

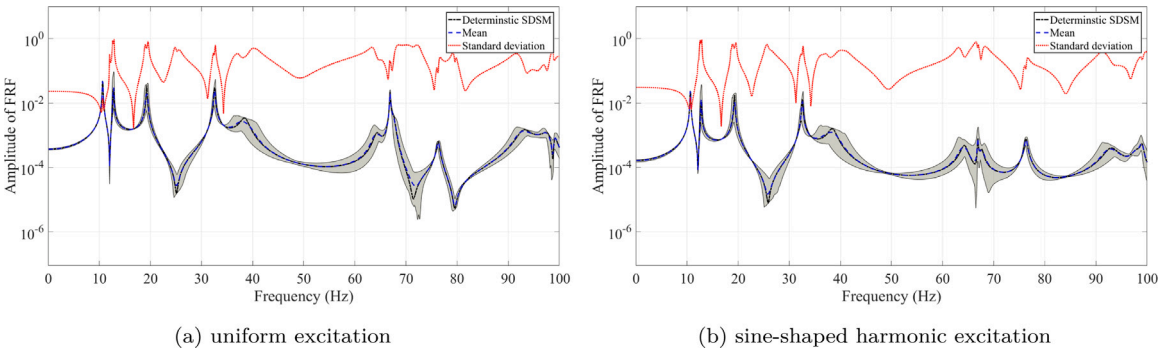

Fig. 9. The amplitudes of dynamic responses at the one point of the free edge shown in Fig. 5 subject to uniform (left) and sine-shaped harmonic (right) excitations. (The gray area represent the responses of the 1000 samples.).

obtain these results, we use a Monte Carlo simulation by generating 1000 samples. We also use direct matrix inversion and domain decomposition method to compute dynamic response and compare the computational time under the same calculation configuration. For the uniform excitations, the direct matrix inversion takes 9748.62 s, and the domain decomposition method takes 6438.26 s. For the case of sine-shaped harmonic excitations, the direct matrix inversion takes 9835.18 s, and the domain decomposition method takes 6511.53 s. It can be seen that the domain decomposition method has obvious computational advantages which is determined by the size of matrix $\boldsymbol{K}_{SS}$ in Eq. (42). The larger the matrices or samples are (The more complex the structure is), the higher obvious the computational efficiency when using the domain decomposition method.

In both cases, the mean of random responses throughout the frequency domain coincides with the deterministic response. Similarly, as for the standard deviations of the responses in the two cases, they are biased by the means and some peaks are reached around the natural frequencies. On the other hand, the dynamic response characteristics of plates with uncertain connection conditions subject to different excitations are also different. In the case of uniform excitation, it can be seen that the frequency domain response will produce scattering near the peak of the curve which is more obvious in the range of 60–75 Hz compared to other ranges. It shows that the stochastic vibration response analysis within 60–75 Hz is worthy of attention subject to uniform excitation. In the case of sine-shaped harmonic excitations, the response will cause scattering only near the peaks of the curve. Comparing with two figures, it can be seen that once the vibration frequency is far away from that corresponding to the peak of the curve, the stochastic response will be close to the deterministic response.

In addition, the mean of the displacement response field is also shown in Fig. 10. Section 6.2.1 has proved the accuracy and efficiency of this method. By combining Figs. 8 and 9, it can be seen that this method is also applicable to uniform and non-uniform boundary conditions and connection conditions.

7. Conclusions

An analytical stochastic spectral dynamic stiffness method (SSDSM) is developed for the dynamic analysis of the plate assembly subject to uncertain viscoelastic boundary or connection conditions (BCs or CCs). In the proposed method, arbitrary spatially-varying deterministic viscoelastic BCs or CCs which includes damping effect are modeled by the spectral dynamic stiffness (SDS) formulations; whereas uncertain viscoelastic BCs or CCs is described by the stochastic SDS formulations. The main novelties of the proposed method include:

- The recently proposed SDS theory has been extended to model plate assembly with arbitrary spatially-varying deterministic viscoelastic BCs or CCs for the broadband vibration analysis.

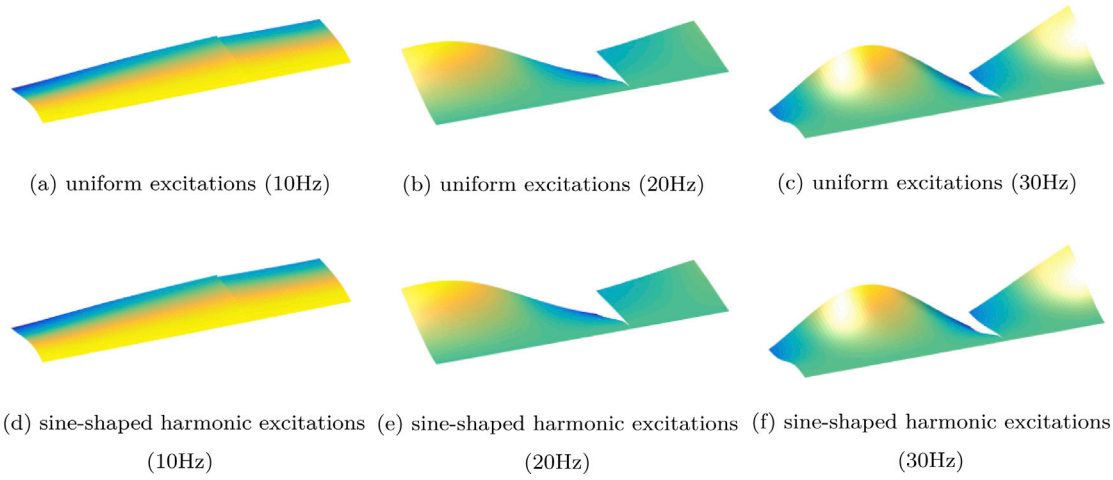

Fig. 10. Mean of displacement response field at three frequencies subject to uniform and sine-shaped harmonic excitations shown in Fig. 8 by using the domain decomposition method.

- An analytical framework for stochastic SDS (SSDS) formulation of the uncertain viscoelastic BCs or CCs (with uncertain stiffness and damping) has been proposed by incorporating the Karhunen–Loève expansion and the extended SDS theory.
- The SSDS matrices are superposed directly to the SDS matrix of plate assembly. The procedure is in a strong form and no extra DOFs are introduced in the final SSDS matrices and therefore, no extra computational effort is required.
- The Wittrick–Williams algorithm and a proposed improved response analysis method are used to compute the stochastic eigenvalues and dynamic responses, which minimizes the computational cost for each random sample, and gives accurate solutions with high computational efficiency.
- The proposed method retains all significant advantages of the SDSM, the accurate and efficient stochastic dynamic analysis can be performed within the whole frequency domain.

Numerical examples are given to illustrate the computational efficiency and accuracy of the proposed method within the whole frequency range. By considering the uncertain stiffness and damping effect of boundary or connection conditions, this method is applicable for stochastic broadband vibration analysis of plate built-up structures subject to mechanical fastening and adhesive bond fastening in the engineering structure design. Furthermore, as a feasible technique for stochastic broadband dynamic analysis, the current research can serve as an efficient, accurate and versatile tool for the uncertainty qualification, model updating [73,74] of uncertain viscoelastic BCs or CCs to the dynamics of complex plate built-up structures.

Declaration of competing interest

The authors declare that they have no known competing financial interests or personal relationships that could have appeared to influence the work reported in this paper.

Acknowledgments

The authors appreciate the supports from National Natural Science Foundation China (Grant No. 11802345), State Key Laboratory of High Performance Complex Manufacturing, China (Grant No. ZZYJKT2019-07), Initial Funding of Specially-appointed Professorship, China (Grant No. 502045001), High-end Foreign Expert Introduction Project, China (Grant No. G2021161001L) which made this research possible.

Appendix A. Modified fourier basis function

The SDSM [64,65,67] combines the spectral (S) method and the classical dynamic stiffness method (DSM). One of the key points in the SDSM lies in adopting a modified Fourier series [69]. The adopted modified Fourier series for any arbitrary displacement or force boundary condition (denoted by $h(\mathrm{r})$) along a plate edge (line node $\mathrm{r} \in [-L, L]$ in local coordinates of plate) is given by

$$h(\mathrm{r}) = \sum_{\substack{s\in\mathbb{N} \\ l\in\{0,1\}}} H_{ls} \frac{\mathcal{T}_l(\gamma_{ls}\mathrm{r})}{\sqrt{\zeta_{ls} L}}, \quad H_{ls} = \int_{-L}^{L} h(\mathrm{r}) \frac{\mathcal{T}_l(\gamma_{ls}\mathrm{r})}{\sqrt{\zeta_{ls} L}} \mathrm{d}\mathrm{r}, \tag{A.1}$$

where $\mathbb{N} = \{0, 1, 2, \ldots\}$ is the non-negative integer set, and the subscript 'l', taking value of either '0' or '1', denotes the corresponding symmetric or antisymmetric functions (and coefficients). Here, ζ_{ls} is given as

$$\zeta_{ls} = \begin{cases} 2 & l = 0 \text{ and } s = 0 \\ 1 & l = 1 \text{ or } s \geq 1 \end{cases}. \tag{A.2}$$

The corresponding modified Fourier basis function $\mathcal{T}_l(\gamma_{ls}\mathrm{r})$ in Eq. (A.1) is defined as

$$\mathcal{T}_l(\gamma_{ls}\mathrm{r}) = \begin{cases} \cos(\frac{s\pi}{L}\mathrm{r}) & l = 0 \\ \sin\left((s+\frac{1}{2})\frac{\pi}{L}\mathrm{r}\right) & l = 1 \end{cases}, \quad \mathrm{r} \in [-L, L], \quad s \in \mathbb{N}, \tag{A.3}$$

which provides a complete and orthogonal set to described any one-dimensional function $h(\mathrm{r})$ of Eq. (A.1) with any arbitrary boundary conditions. It should be emphasized that the above modified Fourier series has strong orthogonality which is one of the most important factors that makes the SDSM numerically stable, therefore any higher order of modified Fourier series can be adopted in the computation to compute results within any desired accuracy. The $\sqrt{\zeta_{ls}L}$ appearing in Eq. (A.1) provides the symmetry of the forward and inverse Fourier transformation. By using the above modified Fourier series, each force $\boldsymbol{f}_i$ and displacement $\boldsymbol{d}_i$ sub-vectors take the following form

$$\boldsymbol{f}_i = \left[F_{i00}, F_{i01}, F_{i02}, \ldots, F_{i10}, F_{i11}, F_{i12}, \ldots\right]^{\mathrm{T}}, \tag{A.4a}$$

$$\boldsymbol{d}_i = \left[D_{i00}, D_{i01}, D_{i02}, \ldots, D_{i10}, D_{i11}, D_{i12}, \ldots\right]^{\mathrm{T}}, \tag{A.4b}$$

where F_{ils} and D_{ils} ($l \in \{0, 1\}, s \in \mathbb{N}$) are respectively the modified Fourier coefficients of the corresponding force $f_i(\mathrm{r})$ and displacement $d_i(\mathrm{r})$ BCs (or CCs) applied on the ith *line DOF* of the plate assembly, which are obtained by applying Eq. (A.1) onto $f_i(\mathrm{r})$ and $d_i(\mathrm{r})$ respectively to give

$$F_{ils} = \int_{-L}^{L} f_i(\mathrm{r}) \frac{\mathcal{T}_l(\gamma_{ls}\mathrm{r})}{\sqrt{\zeta_{ls}L}} \mathrm{d}\mathrm{r}, \tag{A.5a}$$

$$D_{ils} = \int_{-L}^{L} d_i(\mathrm{r}) \frac{\mathcal{T}_l(\gamma_{ls}\mathrm{r})}{\sqrt{\zeta_{ls}L}} \mathrm{d}\mathrm{r}. \tag{A.5b}$$

Therefore, each term of either F_{ils} or D_{ils} in Eq. (A.5) represents a frequency–wavenumber dependent DOF of the ith *line DOF*. Following the definitions given in Eqs. (A.1) to (A.3), the subscript 'l' in Eq. (A.5), being '0' or '1', stands respectively for the modified Fourier cosine (for symmetric component) or sine (for antisymmetric component) coefficients of the ith *line DOF*. Therefore, the BCs (or CCs) can be arbitrarily prescribed along any *line DOFs*, which are directly transformed through Eq. (A.5) into vector form (i.e., $\boldsymbol{f}_i$ and $\boldsymbol{d}_i$) of Eq. (A.4) and eventually into $\boldsymbol{f}$ and $\boldsymbol{d}$ in Eq. (4).

Appendix B. The modified fourier form of excitation

This appendix includes the analytical expressions of the $\boldsymbol{F}$ vector only for some typical spatially functions $F^b(\mathrm{r})$. For the sake of notational convenience, some notations are introduced. $[.]_{S-1}$ stands for a row vector with '.' taking $s \in [0, S-1]$. And $\boldsymbol{F}_0$ and $\boldsymbol{F}_1$ are two parts of $\boldsymbol{F}$ vector, whose combined form is $\boldsymbol{F} = [\boldsymbol{F}_0; \boldsymbol{F}_1]$.

(1) For constant function $F^b(\mathrm{r}) = 1$, $\boldsymbol{F}_0 = [\sqrt{2L}, [0]_{S-1}]$, $\boldsymbol{F}_1 = [[0]_S]$

(2) For parabolic function $F^b(\mathrm{r}) = (\frac{\mathrm{r}}{L})^2$, $\boldsymbol{F}_0 = [\frac{\sqrt{2L}}{3}, [\frac{4(-1)^s\sqrt{L}}{\pi^2 s^2}]_{S-1}]$, $\boldsymbol{F}_1 = [[0]_S]$

(3) For cosine function $F^b(\mathrm{r}) = \cos\left[\frac{\pi\mathrm{r}}{2L}\right]$, $\boldsymbol{F}_0 = [\frac{2\sqrt{2L}}{\pi}, \quad [\frac{4(-1)^s\sqrt{L}}{\pi - 4\pi s^2}]_{S-1}]$, $\boldsymbol{F}_1 = [[0]_S]$

(4) For sine function $F^b(\mathrm{r}) = \sin\left[\frac{\pi\mathrm{r}}{2L}\right]$, $\boldsymbol{F}_0 = [0, [0]_{S-1}]$, $\boldsymbol{F}_1 = [[0]_S]$

(5) For linear function $F^b(\mathrm{r}) = \frac{L+\mathrm{r}}{L}$, $\boldsymbol{F}_0 = [\sqrt{2L}, [0]_{S-1}]$, $\boldsymbol{F}_1 = [[\frac{8(-1)^s\sqrt{L}}{(\pi+2\pi s)^2}]_S]$

$F^b(\mathrm{r}) = \frac{L-\mathrm{r}}{L}$, $\boldsymbol{F}_0 = [\sqrt{2L}, [0]_{S-1}]$, $\boldsymbol{F}_1 = [[-\frac{8(-1)^s\sqrt{L}}{(\pi+2\pi s)^2}]_S]$

$F^b(\mathrm{r}) = \frac{3L+\mathrm{r}}{L}$, $\boldsymbol{F}_0 = [3\sqrt{2L}, [0]_{S-1}]$, $\boldsymbol{F}_1 = [[-\frac{8(-1)^s\sqrt{L}}{(\pi+2\pi s)^2}]_S]$

References

[1] R. Gao, Y. Zhang, D. Kennedy, Optimization of mid-frequency vibration for complex built-up systems using the hybrid finite element–statistical energy analysis method, Eng. Optim. 52 (12) (2020) 2125–2145, http://dx.doi.org/10.1080/0305215X.2019.1691546.

[2] R. Gao, Y. Zhang, D. Kennedy, Application of the dynamic condensation approach to the hybrid FE-SEA model of mid-frequency vibration in complex built-up systems, Comput. Struct. 228 (2020) 106156, http://dx.doi.org/10.1016/j.compstruc.2019.106156.

[3] R.A. Ibrahim, C.L. Pettit, Uncertainties and dynamic problems of bolted joints and other fasteners, J. Sound Vib. 279 (3–5) (2005) 857–936, http://dx.doi.org/10.1016/j.jsv.2003.11.064.

[4] D.K. Wilson, C.L. Pettit, V.E. Ostashev, S.N. Vecherin, Description and quantification of uncertainty in outdoor sound propagation calculations, J. Acoust. Soc. Am. 136 (3) (2014) 1013–1028, http://dx.doi.org/10.1121/1.4890644.

[5] S. Sarkar, D. Ghosh, A hybrid method for stochastic response analysis of a vibrating structure, Arch. Appl. Mech. 85 (11) (2015) 1607–1626, http://dx.doi.org/10.1007/s00419-015-1007-6.

[6] W.J. Yan, L.S. Katafygiotis, An analytical investigation into the propagation properties of uncertainty in a two-stage fast Bayesian spectral density approach for ambient modal analysis, Mech. Syst. Signal Process. 118 (2019) 503–533, http://dx.doi.org/10.1016/j.ymssp.2018.08.047.

[7] G. Chen, D. Yang, Direct probability integral method for stochastic response analysis of static and dynamic structural systems, Comput. Methods Appl. Mech. Engrg. 357 (2019) 112612, http://dx.doi.org/10.1016/j.cma.2019.112612.

[8] D. Yang, P. Yi, Chaos control of performance measure approach for evaluation of probabilistic constraints, Struct. Multidiscip. Optim. 38 (1) (2009) 83–92, http://dx.doi.org/10.1007/s00158-008-0270-3.

[9] C.L. Pettit, M.R. Hajj, P.S. Beran, A stochastic approach for modeling incident gust effects on flow quantities, Probab. Eng. Mech. 25 (1) (2010) 153–162, http://dx.doi.org/10.1016/j.probengmech.2009.08.007.

[10] N.J. Lindsley, C.L. Pettit, P.S. Beran, Nonlinear plate aeroelastic response with uncertain stiffness and boundary conditions, Struct. Infrastruct. Eng. 2 (3–4) (2006) 201–220, http://dx.doi.org/10.1080/15732470600590564.

[11] G.M. Castelluccio, M.R.W. Brake, On the origin of computational model sensitivity, error, and uncertainty in threaded fasteners, Comput. Struct. 186 (2017) 1–10, http://dx.doi.org/10.1016/j.compstruc.2017.03.004.

[12] B. Huang, Q.S. Li, W.H. Shi, Z. Wu, Eigenvalues of structures with uncertain elastic boundary restraints, Appl. Acoust. 68 (3) (2007) 350–363, http://dx.doi.org/10.1016/j.apacoust.2006.01.012.

[13] G.L.S. Silva, D.A. Castello, L. Borges, J.P. Kaipio, Damage identification in plates under uncertain boundary conditions, Mech. Syst. Signal Process. 144 (2020) 106884, http://dx.doi.org/10.1016/j.ymssp.2020.106884.

[14] H. Li, H. Lv, H. Sun, Z. Qin, J. Xiong, Q. Han, J. Liu, X. Wang, Nonlinear vibrations of fiber-reinforced composite cylindrical shells with bolt loosening boundary conditions, J. Sound Vib. 496 (2021) 115935, http://dx.doi.org/10.1016/j.jsv.2021.115935.

[15] S.L. Qiao, V.N. Pilipchuk, R.A. Ibrahim, Modeling and simulation of elastic structures with parameter uncertainties and relaxation of joints, Trans. ASME. J. Vib. Acoust. 123 (1) (2001) 45–52, http://dx.doi.org/10.1115/1.1325409.

[16] M. Dilena, M.F. Dell'Oste, A. Morassi, Crack identification in rods and beams under uncertain boundary conditions, Int. J. Mech. Sci. 133 (August) (2017) 651–661, http://dx.doi.org/10.1016/j.ijmecsci.2017.09.017.

[17] U. Lee, J. Kim, Determination of nonideal beam boundary conditions: A spectral element approach, AIAA J. 38 (2) (2000) 309–316, http://dx.doi.org/10.2514/2.958.

[18] T.G. Ritto, R. Sampaio, E. Cataldo, Timoshenko Beam with uncertainty on the boundary conditions, J. Braz. Soc. Mech. Sci. Eng. 30 (4) (2008) 295–303, http://dx.doi.org/10.1590/S1678-58782008000400005.

[19] L. Dozio, On the use of the trigonometric Ritz method for general vibration analysis of rectangular Kirchhoff plates, Thin-Walled Struct. 49 (1) (2011) 129–144, http://dx.doi.org/10.1016/j.tws.2010.08.014.

[20] W.L. Li, Vibration analysis of rectangular plates with general elastic boundary supports, J. Sound Vib. 273 (3) (2004) 619–635, http://dx.doi.org/10.1016/S0022-460X(03)00562-5.

[21] Y.K. Cheung, D. Zhou, Vibrations of rectangular plates with elastic intermediate line-supports and edge constraints, Thin-Walled Struct. 37 (4) (2000) 305–331, http://dx.doi.org/10.1016/S0263-8231(00)00015-X.

[22] D. Zhou, Natural frequencies of elastically restrained rectangular plates using a set of static beam functions in the Rayleigh-Ritz method, Comput. Struct. 57 (4) (1995) 731–735, http://dx.doi.org/10.1016/0045-7949(95)00066-P.

[23] S.A. Eftekhari, A.A. Jafari, Accurate variational approach for free vibration of variable thickness thin and thick plates with edges elastically restrained against translation and rotation, Int. J. Mech. Sci. 68 (2013) 35–46, http://dx.doi.org/10.1016/j.ijmecsci.2012.12.012.

[24] L.G. Nallim, R.O. Grossi, Vibration of angle-ply symmetric laminated composite plates with edges elastically restrained, Compos. Struct. 81 (1) (2007) 80–83, http://dx.doi.org/10.1016/j.compstruct.2006.07.012.

[25] H. Khov, W.L. Li, R.F. Gibson, An accurate solution method for the static and dynamic deflections of orthotropic plates with general boundary conditions, Compos. Struct. 90 (4) (2009) 474–481, http://dx.doi.org/10.1016/j.compstruct.2009.04.020.

[26] D. Stăncioiu, H. Ouyang, J.E. Mottershead, Vibration of a continuous beam with multiple elastic supports excited by a moving two-axle system with separation, Meccanica 44 (3) (2009) 293–303, http://dx.doi.org/10.1007/s11012-008-9172-0.

[27] M. Oldfield, H. Ouyang, J.E. Mottershead, Simplified models of bolted joints under harmonic loading, Comput. Struct. 84 (1–2) (2005) 25–33, http://dx.doi.org/10.1016/j.compstruc.2005.09.007.

[28] M. Ceberio, V. Kreinovich, Decision Making under Contraints, 2020.

[29] J. Avalos, L.A. Richter, X.Q. Wang, R. Murthy, M.P. Mignolet, Stochastic modal models of slender uncertain curved beams preloaded through clamping, J. Sound Vib. 334 (2015) 363–376, http://dx.doi.org/10.1016/j.jsv.2014.08.037.

[30] T.G. Ritto, R. Sampaio, R.R. Aguiar, Uncertain boundary condition Bayesian identification from experimental data: A case study on a cantilever beam, Mech. Syst. Signal Process. 68–69 (2016) 176–188, http://dx.doi.org/10.1016/j.ymssp.2015.08.010.

[31] A. Abolfathi, D.J. O'Boy, S.J. Walsh, S.A. Fisher, Investigating the sources of variability in the dynamic response of built-up structures through a linear analytical model, J. Sound Vib. 387 (2017) 163–176, http://dx.doi.org/10.1016/j.jsv.2016.10.007.

[32] H. Jalali, H.H. Khodaparast, H. Madinei, M.I. Friswell, Stochastic modelling and updating of a joint contact interface, Mech. Syst. Signal Process. 129 (2019) 645–658, http://dx.doi.org/10.1016/j.ymssp.2019.04.003.

[33] M.P. Mignolet, C. Soize, Nonparametric stochastic modeling of structural dynamic systems with uncertain boundary conditions, 2007.

[34] C. López, A. Baldomir, E. Menga, S. Hernández, C. Cid, D. Freire, A study of uncertainties in dynamic properties of assembled aircraft structures, in: Proceedings of ISMA 2016 - International Conference on Noise and Vibration Engineering and USD2016 - International Conference on Uncertainty in Structural Dynamics, 2016, pp. 4447–4461.

[35] M. Marc, C. Soize, J. Avalos, Nonparametric stochastic modeling of structures with uncertain boundary conditions/coupling between substructures, AIAA J. 51 (6) (2013) 1296–1308, http://dx.doi.org/10.2514/1.J051555.

[36] G. Jin, T. Ye, X. Ma, Y. Chen, Z. Su, X. Xie, A unified approach for the vibration analysis of moderately thick composite laminated cylindrical shells with arbitrary boundary conditions, Int. J. Mech. Sci. 75 (2013) 357–376, http://dx.doi.org/10.1016/j.ijmecsci.2013.08.003.

[37] Y. Zhou, Q. Wang, D. Shi, Q. Liang, Z. Zhang, Exact solutions for the free in-plane vibrations of rectangular plates with arbitrary boundary conditions, Int. J. Mech. Sci. 130 (932) (2017) 1339–1351, http://dx.doi.org/10.1016/j.ijmecsci.2017.06.004.

[38] Q. Song, J. Shi, Z. Liu, Y. Wan, Dynamic analysis of rectangular thin plates of arbitrary boundary conditions under moving loads, Int. J. Mech. Sci. 117 (2016) 16–29, http://dx.doi.org/10.1016/j.ijmecsci.2016.08.005.

[39] X. Shi, D. Shi, W.L. Li, Q. Wang, A unified method for free vibration analysis of circular, annular and sector plates with arbitrary boundary conditions, J. Vib. Control 22 (2) (2016) 442–456, http://dx.doi.org/10.1177/1077546314533580.

[40] H. Li, H. Lv, H. Sun, Z. Qin, J. Xiong, Q. Han, J. Liu, X. Wang, Nonlinear vibrations of fiber-reinforced composite cylindrical shells with bolt loosening boundary conditions, J. Sound Vib. 496 (2021) 115935, http://dx.doi.org/10.1016/j.jsv.2021.115935.

[41] S. Adhikari, Doubly spectral stochastic finite-element method for linear structural dynamics, J. Aerosp. Eng. 24 (3) (2011) 264–276, http://dx.doi.org/10.1061/(ASCE)AS.1943-5525.0000070.

[42] X. Liu, X. Zhao, S. Adhikari, X. Liu, Stochastic dynamic stiffness for damped taut membranes, Comput. Struct. (2021) 1–29, http://dx.doi.org/10.1016/j.compstruc.2021.106483.

[43] J.R. Banerjee, Review of the dynamic stiffness method for free-vibration analysis of beams, Transp. Saf. Environ. 1 (2) (2019) 106–116, http://dx.doi.org/10.1093/tse/tdz005.
[44] J.R. Banerjee, A. Ananthapuvirajah, An exact dynamic stiffness matrix for a beam incorporating Rayleigh–Love and Timoshenko theories, Int. J. Mech. Sci. 150 (June 2018) (2019) 337–347, http://dx.doi.org/10.1016/j.ijmecsci.2018.10.012.
[45] X. Liu, X. Zhao, C. Xie, Exact free vibration analysis for membrane assemblies with general classical boundary conditions, J. Sound Vib. 485 (2020) 115484, http://dx.doi.org/10.1016/j.jsv.2020.115484.
[46] J.R. Banerjee, Extension of the wittrick-williams algorithm for free vibration analysis of hybrid dynamic stiffness models connecting line and point nodes, Mathematics 10 (2021).
[47] X. Liu, Y. Zhao, W. Zhou, J.R. Banerjee, Dynamic stiffness method for exact longitudinal free vibration of rods and trusses using simple and advanced theories, Appl. Math. Model. 104 (2022) 401–420.
[48] X. Liu, X. Liu, S. Xie, A highly accurate analytical spectral flexibility formulation for buckling and wrinkling of orthotropic rectangular plates, Int. J. Mech. Sci. 168 (2020) 105311.
[49] X. Liu, X. Liu, W. Zhou, An analytical spectral stiffness method for buckling of rectangular plates on Winkler foundation subject to general boundary conditions, Appl. Math. Model. 86 (2020) 36–53.
[50] X. Liu, X. Zhao, S. Adhikari, X. Liu, Stochastic dynamic stiffness for damped taut membranes, Comput. Struct. 248 (2021) 106483.
[51] X. Liu, L. Chang, J.R. Banerjee, H.-C. Dan, Closed-form dynamic stiffness formulation for exact modal analysis of tapered and functionally graded beams and their assemblies, Int. J. Mech. Sci. 214 (2022) 106887.
[52] X. Liu, C. Sun, J. Ranjan Banerjee, H.C. Dan, L. Chang, An exact dynamic stiffness method for multibody systems consisting of beams and rigid-bodies, Mech. Syst. Signal Process. 150 (2021) 107264, http://dx.doi.org/10.1016/j.ymssp.2020.107264.
[53] X. Liu, Y. Li, Y. Lin, J.R. Banerjee, Spectral dynamic stiffness theory for free vibration analysis of plate structures stiffened by beams with arbitrary cross-sections, Thin-Walled Struct. 160 (June 2020) (2021) http://dx.doi.org/10.1016/j.tws.2020.107391.
[54] X. Liu, C. Xie, H.C. Dan, Exact free vibration analysis for plate built-up structures under comprehensive combinations of boundary conditions, Shock Vib. 2020 (2020) http://dx.doi.org/10.1155/2020/5305692.
[55] X. Liu, J.R. Banerjee, A spectral dynamic stiffness method for free vibration analysis of plane elastodynamic problems, Mech. Syst. Signal Process. 87 (2017) 136–160, http://dx.doi.org/10.1016/j.ymssp.2016.10.017.
[56] X. Liu, X. Liu, S. Adhikari, S. Yin, Extended wittrick–williams algorithm for eigenvalue solution of stochastic dynamic stiffness method, Mech. Syst. Signal Process. 166 (September 2021) (2022) 108354, http://dx.doi.org/10.1016/j.ymssp.2021.108354.
[57] M.R. Machado, S. Adhikari, J.M.C. Santos, A spectral approach for damage quantification in stochastic dynamic systems, Mech. Syst. Signal Process. 88 (June 2016) (2017) 253–273, http://dx.doi.org/10.1016/j.ymssp.2016.11.018.
[58] W.H. Wittrick, Buckling and vibration of anisotropic or isotropic plate assemblies under combined loadings, Int. J. Mech. Sci. 16 (4) (1974) 209–239.
[59] M. Boscolo, J.R. Banerjee, Dynamic stiffness elements and their applications for plates using first order shear deformation theory, Comput. Struct. 89 (3–4) (2011) 395–410, http://dx.doi.org/10.1016/j.compstruc.2010.11.005.
[60] M. Boscolo, J.R. Banerjee, Dynamic stiffness formulation for composite Mindlin plates for exact modal analysis of structures . Part I : Theory, Comput. Struct. 96–97 (2012) 61–73, http://dx.doi.org/10.1016/j.compstruc.2012.01.002.
[61] M. Boscolo, J.R. Banerjee, Dynamic stiffness formulation for composite Mindlin plates for exact modal analysis of structures . Part II : Results and applications, Comput. Struct. 96–97 (2012) 74–83, http://dx.doi.org/10.1016/j.compstruc.2012.01.003.
[62] F.A. Fazzolari, M. Boscolo, J.R. Banerjee, An exact dynamic stiffness element using a higher order shear deformation theory for free vibration analysis of composite plate assemblies, Compos. Struct. 96 (2013) 262–278, http://dx.doi.org/10.1016/j.compstruct.2012.08.033.
[63] M. Boscolo, J.R. Banerjee, Layer-wise dynamic stiffness solution for free vibration analysis of laminated composite plates, J. Sound Vib. 333 (1) (2014) 200–227, http://dx.doi.org/10.1016/j.jsv.2013.08.031.
[64] X. Liu, J.R. Banerjee, An exact spectral-dynamic stiffness method for free flexural vibration analysis of orthotropic composite plate assemblies - part I: Theory, Compos. Struct. 132 (2015) 1274–1287, http://dx.doi.org/10.1016/j.compstruct.2015.07.020.
[65] X. Liu, J.R. Banerjee, An exact spectral-dynamic stiffness method for free flexural vibration analysis of orthotropic composite plate assemblies - part II: Applications, Compos. Struct. 132 (2015) 1288–1302, http://dx.doi.org/10.1016/j.compstruct.2015.07.022.
[66] X. Liu, H.I. Kassem, J.R. Banerjee, An exact spectral dynamic stiffness theory for composite plate-like structures with arbitrary non-uniform elastic supports, mass attachments and coupling constraints, Compos. Struct. 142 (2016) 140–154, http://dx.doi.org/10.1016/j.compstruct.2016.01.074.
[67] X. Liu, J.R. Banerjee, Free vibration analysis for plates with arbitrary boundary conditions using a novel spectral-dynamic stiffness method, Comput. Struct. 164 (2016) 108–126, http://dx.doi.org/10.1016/j.compstruc.2015.11.005.
[68] S. Pranesh, D. Ghosh, Faster computation of the karhunen-loève expansion using its domain independence property, Comput. Methods Appl. Mech. Engrg. 285 (2015) 125–145, http://dx.doi.org/10.1016/j.cma.2014.10.053.
[69] A. Iserles, S.P. Nørsett, From high oscillation to rapid approximation I : Modified Fourier expansions, 28 (2008) 862–887, http://dx.doi.org/10.1093/imanum/drn006.
[70] R. Ghanem, P.D. Spanos, Stochastic Finite Elements: A Spectral Approach, Springer-Verlag, New York, USA, 1991.
[71] A. Papoulis, S.U. Pillai, Probability, Random Variables and Stochastic Processes, Fourth, McGraw-Hill, Boston, USA, 2002.
[72] F.W. Williams, A general algorithm for computing natural frequencies of elastic structures, XXIV (September 1970) (1971).
[73] H.H. Khodaparast, J.E. Mottershead, K.J. Badcock, Interval model updating with irreducible uncertainty using the Kriging predictor, Mech. Syst. Signal Process. 25 (4) (2011) 1204–1226, http://dx.doi.org/10.1016/j.ymssp.2010.10.009.
[74] W.J. Yan, S.Z. Cao, W.X. Ren, K.V. Yuen, D. Li, L. Katafygiotis, Vectorization and distributed parallelization of Bayesian model updating based on a multivariate complex-valued probabilistic model of frequency response functions, Mech. Syst. Signal Process. 156 (2021) 107615, http://dx.doi.org/10.1016/j.ymssp.2021.107615.